JOC The Journal of Organic Chemistry

Article

pubs.acs.org/joc

Chemoenzymatic Synthesis of Proxyphylline Enantiomers

Paweł Borowiecki,*[,†] Daniel Paprocki,[†] Agnieszka Dudzik,[‡] and Jan Plenkiewicz[†]

[†]Warsaw University of Technology, Faculty of Chemistry, Institute of Biotechnology, Koszykowa St. 3, 00-664 Warsaw, Poland

[‡]Jerzy Haber Institute of Catalysis and Surface Chemistry, Polish Academy of Sciences, Niezapominajek St. 8, 30-239 Cracow, Poland

Supporting Information

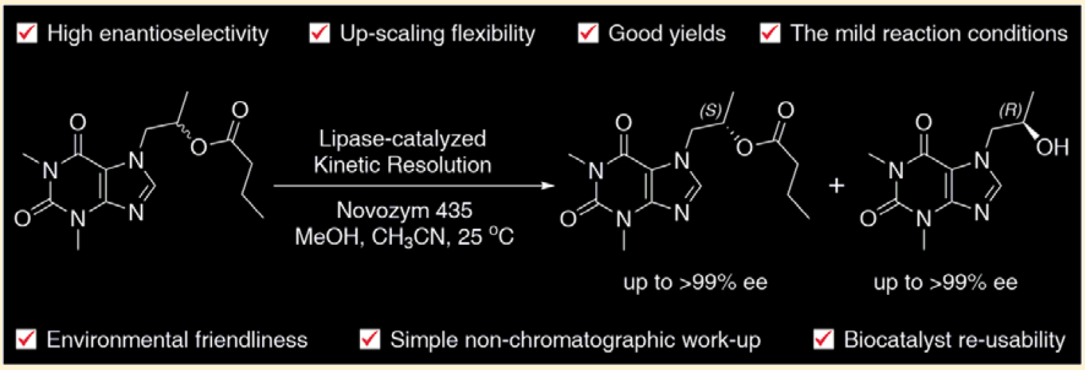

ABSTRACT: A novel synthetic route for preparation of proxyphylline enantiomers using a kinetic resolution (KR) procedure as the key step is presented. The reactions were catalyzed by immobilized *Candida antarctica* lipase B in acetonitrile. Three types of reactions were examined: (i) enantioselective transesterification of racemic proxyphylline with vinyl acetate as well as (ii) hydrolysis and (iii) methanolysis of its esters. The influence of reaction conditions on the substrate conversion and enantiomeric purity of the products were investigated. Studies on analytical scale reactions revealed that the titled API enantiomers could be successfully obtained with excellent enantiomeric excess (up to >99% ee). The process was easily conducted on a 5 g scale at 100 g/L. In a preparative-scale reaction, unreacted (*S*)-(+)-butanoate (97% ee) and (*R*)-(−)-alcohol (96% ee) were obtained after 2 days in yields of 45% and 46%, respectively. When the reaction time was extended to 6 days, (*S*)-(+)-butanoate was isolated in >99% ee and acceptable high enantioselectivity (E = 90). Importantly, the KR's products could be conveniently isolated by exploiting varying solubility of the ester/alcohol in acetonitrile at room temperature. In addition, a chiral preference of the CAL-B active site for the *R*-enantiomer was rationalized by *in sillico* docking studies.

1. INTRODUCTION

Chirality is one of the immanent characteristics of nature and plays a key role in metabolic processes as well as in many areas of science and technology.[1] Therefore, synthesis of enantiomerically pure drugs is of prime concern for medicinal chemistry, especially as single stereoisomers of active pharmaceutical ingredients (APIs) can act differently in living systems such as human beings or pathogens.[2] This stems mainly from particular stereoselective interactions at biological receptors (enzymes, hormones etc.), which are built up of chiral molecules, such as amino acids, sugars, and steroids. In order to avert adverse side effects that may pose danger to a patient's life, application of chiral pharmaceuticals should have been preceded by thorough biological and clinical evaluations conducted on both the racemate and its respective enantiomers.[3] Moreover, administering chiral substances as single enantiomers diminishes the amount of drug to achieve the expected therapeutic effect. For this reason, a vast number of racemate separation techniques[4] including direct preferential crystallization of enantiomeric mixtures (homo- and heterochiral aggregates), fractional crystallization of diastereomeric salts (classical resolution), chromatography on chiral phases, and kinetic resolution mediated by chiral selectors/auxiliaries are essential prerequisites to prepare compounds in enantiomerically pure forms or at least in a very high enantioenrichment. Among the aforementioned procedures, especially protocols employing enzymes as catalysts for kinetic resolution of enantiomers have passed to the canon of synthetic organic chemistry as one of the most elegant and sustainable strategies.

Hydrolases are the most commonly employed enzymes, which has received great attention these days.[5] Among the hydrolytic enzymes, lipases (triacylglycerol ester hydrolases, EC 3.1.1.3) are beyond any doubt the most versatile and practical biocatalysts used in organic chemistry[6] due to their selectivity in action, wide substrate specificity, commercial availability in both free and immobilized forms, low price, easy handling, high reaction rates, and ability to retain almost full catalytic activity even in nearly anhydrous organic solvents,[7] in nonconventional media such as neoteric solvents [i.e., ionic liquids (ILs), supercritical carbon dioxide ($scCO_2$), fluorous solvents (FSs), and liquid polymers (LPs)],[8] and in solvent-free systems.[9]

Received: August 13, 2015
Published: October 30, 2015

DOI: 10.1021/acs.joc.5b01840
J. Org. Chem. 2016, 81, 380−395

Scheme 1. Chemoenzymatic Synthesis of Both Enantiomers of Proxyphylline (*S*)-(+)-3 and (*R*)-(−)-3[a]

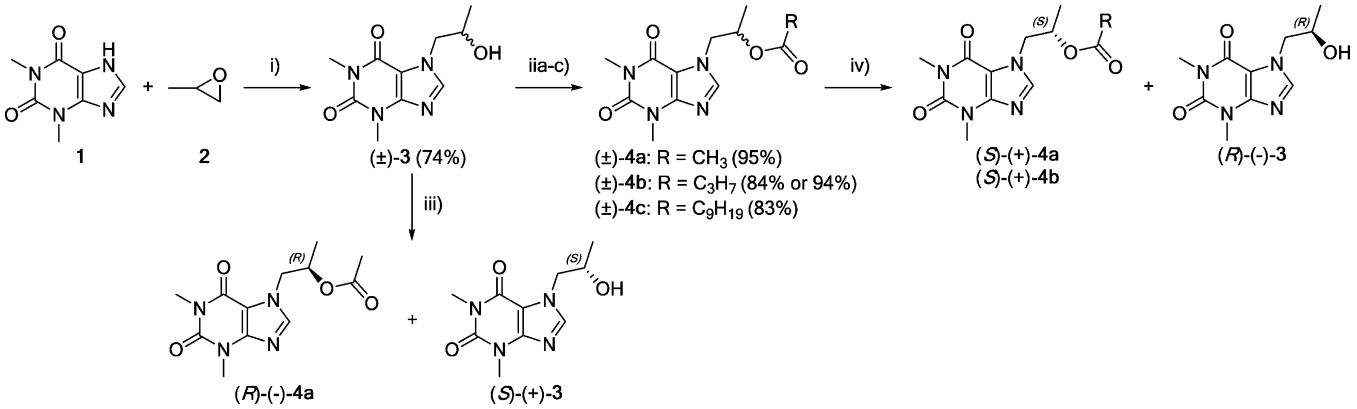

[a]Reagents and conditions: (i) propylene oxide **2** (2 equiv), Et_3N (cat.), MeOH, 4 h at reflux; (iia) Ac_2O (6.5 equiv), DMAP (0.2 equiv), dry CH_2Cl_2, 12 h at rt; (iib) C_3H_7COCl (1.5 equiv) or $C_9H_{19}COCl$ (1.5 equiv), NEt_3 (1.5 equiv), DMAP (0.1 equiv), dry CH_2Cl_2, 12 h at rt; (iic) vinyl butanoate (4.5 equiv), Novozym 435 (5% w/w), MTBE, 12 h at rt, 1000 rpm; (iii) lipase-catalyzed transesterification: vinyl ester, lipase (20% w/w), solvent, 25 °C, 500 rpm; (iv) lipase-catalyzed hydrolysis/methanolysis: H_2O or Tris-HCl Buffer/MeOH, lipase, solvent, 25 °C, 500 rpm.

Moreover, reactions catalyzed by lipases can be carried out: at high substrate concentration (this prevents misusing of organic solvents and thus improve waste-solvent management), without usage of expensive cofactors, and in ordinary stirred tank reactors (what eliminate restructuring requirements of the conventional chemical apparatus). Lipases can also catalyze transformations of sensitive substrates or complex reactions, for which standard chemical methods are not accessible. Last but not least, it is well documented that lipases are also capable of catalyzing asymmetric and nonasymmetric carbon−carbon bond formation which become attractive as very promising alternatives to more traditional synthetic routes.[10] Apart from improving important bond-forming reactions, so-called "lipase promiscuity" can also allow development of new types of reactivity, which can be exploited to provide shorter and more efficient reaction pathways.

Besides the above-mentioned characteristics, a number of important developments have helped to increase the utility of lipases, including protein engineering,[11] protein purification methods,[12] and immobilization techniques,[13] which improve enzyme stability, activity, and enantioselectivity as well as allow simple catalyst recovery, thereby influencing the overall efficiency of the reactions. In this context, lipases serve as highly valuable and efficient catalysts for numerous applications including modification of fats and oils;[14] synthesis of pharmaceuticals,[15] agrochemicals,[16] natural products,[17] vitamins,[18] cosmetics,[19] fragrances and flavors;[20] and preparation of modified foods additives,[21] nutraceuticals,[22] detergents,[23] biodegradable polymers,[24] advanced materials,[25] and biodiesel.[26] In addition, the usage of lipases in the processing of renewable raw materials,[27] in disposing of waste oils and lubricants,[28] and in biodegradation of toxic xenobiotics[29] is also steadily increasing.

Although lipases are broadly applicable biocatalysts for enantioselective transesterification of structurally different secondary alcohols;[30] direct esterification of carboxylic acids;[31] hydrolysis of esters,[32] amides,[33] and lactams;[34] desymmetrization of prochiral diols/diesters,[35] *meso*-1,2-diamines,[36] and pentane-1,5-diamines;[37] and stereoselective synthesis of *sec*-amines and amino acid derivatives,[38] to the best of our knowledge, hydrolytic enzymes of this type have not been used toward 1,3-dimethylxanthines until now. Moreover, according to the literature, optical resolution of proxyphylline was achieved only for its diastereoisomeric camphanates and carried out by thin-layer chromatography (TLC) and fractional crystallization from methanol[39] or reversed-phase liquid chromatography[40] mainly for analytical purposes. In this paper, we present the simple and efficient chemoenzymatic synthesis of both proxyphylline enantiomers in a preparative scale.

2. RESULTS AND DISCUSSION

2.1. Synthesis of Racemic Proxyphylline (±)-3 and Its Esters (±)-4a−c. The principal objective of this work was to develop a simple and efficient chemoenzymatic procedure for the sustainable synthesis of a well-known pharmaceutically valuable compound with cardiac stimulant, vasodilator, and bronchodilator activities—proxyphylline [(±)-**3**, 7-(2-hydroxypropyl)-1,3-dimethyl-3,7-dihydro-1*H*-purine-2,6-dione]. In the first step, racemic starting material (±)-**3** was synthesized by triethylamine-mediated regioselective ring opening of propylene oxide **2** with theophylline (**1**, 1,3-dimethyl-7*H*-purine-2,6-dione) in boiling methanol (Scheme 1). The reaction proceeded smoothly, and after 4 h, and recrystallization from methanol, the product (±)-**3** was prepared in good 74% yield. Interestingly, despite the fact that proxyphylline has been widely used in clinical practice for over 60 years,[41] the nuclear magnetic resonance spectra of (±)-**3** have not been reported until now. Next, to obtain racemic esters (±)-**4a−c** requested for the preparative enzymatic hydrolysis/methanolysis attempts and robust analytical studies of high performance liquid chromatography (HPLC) separation, the afore-prepared alcohol (±)-**3** was treated with acetic anhydride or with the appropriate acyl chloride in dry dichloromethane in the presence of triethylamine and a catalytic amount of 4-(*N*,*N*)-dimethylaminopyridine (DMAP). Under "classical" esterification conditions, esters (±)-**4a−c** could be synthesized in high yields (83−95%).

Notably, during the course of this study we have observed a quite interesting phenomenon regarding spontaneous polymorphic transformation of one of the racemic esters. Chromatographic purification and subsequent recrystallization of the acetate (±)-**4a** from methanol yielded three independent crops of crystalline solids of different, but very narrow, melting

DOI: 10.1021/acs.joc.5b01840
J. Org. Chem. 2016, 81, 380−395

Table 1. Lipase Screening for the Enantioselective *O*-Acetylation of (±)-3 under Kinetically Controlled Conditions in $CHCl_3$

Entry	Lipase preparation[a]	*t* [d]	Conv. [%]	ee_s[b] [%]/(config.)	ee_p[c] [%]/(config.)	*E*[d]
1	Novozym 435	2	53[e]	59/(*S*)	52/(*R*)	6
2	Chirazyme L-2, C-2	2	37[e]	35/(*S*)	59/(*R*)	5
3	Chirazyme L-2, C-3	1	26[e]	18/(*S*)	52/(*R*)	4
4	Amano PS	7	5[f]	N.D.[g]	N.D.[g]	N.D.[g]
5	Amano PS-IM	7	19[e]	18/(*S*)	76/(*R*)	9
6	Amano AK	1	0	N.D.[g]	N.D.[g]	N.D.[g]
7	Lipozyme TL IM	1	30[e]	13/(*S*)	30/(*R*)	2
8	Lipozyme RM IM	1	0	N.D.[g]	N.D.[g]	N.D.[g]

[a]Conditions: (±)-**3** 100 mg, lipase 20 mg, $CHCl_3$ 1 mL, vinyl acetate 415 mg, 0.5 mL (11.5 equiv), 25 °C, 500 rpm (magnetic stirrer). [b]Determined by chiral HPLC analysis of corresponding alcohol obtained after derivatization of alcohol (*S*)-(+)-**3** into the corresponding acetate (*S*)-(+)-**4a**, which was performed by addition of DMAP and Ac_2O (5 equiv) since direct analysis of (*S*)-(+)-**3** with Chiralcel OD-H column was unsatisfactory. [c]Determined by chiral HPLC analysis by using a Chiralcel OD-H column. [d]Calculated according to Chen et al.,[42] using the equation: $E = \{\ln[(1 - \text{conv.})(1 - ee_s)]\}/\{\ln[(1 - \text{conv.})(1 + ee_s)]\}$. [e]Based on GC, for confirmation the % conversion was calculated from the enantiomeric excess of the unreacted alcohol (ee_s) and the product (ee_p) according to the formula conv. = $ee_s/(ee_s + ee_p)$. [f]Based on gas chromatography (GC). [g]Not determined.

point ranges, respectively. At first, we thought that fractions of those products are structurally different, although after analysis it turned out that all these solids are different crystalline structures of proxyphilline acetate (±)-**4a**. This feature might be considered very interesting from a pharmaceutical point of view due to its potential influence on drug processing as well as drug quality, safety, and overall performance since the pharmacokinetics, delivery, and bioavailability of biologically active substances is significantly dependent on crystal polymorphism.

Moreover, surprisingly if the alcohol (±)-**3** was treated with vinyl butanoate in the presence of Novozym 435 suspended in methyl *tert*-butyl ether (MTBE), and vigorously stirred (1000 rpm) at room temperature overnight, *O*-butyryl ester (±)-**4b** was afforded in excellent yield (94%) under mild reaction conditions. Although substrate (±)-**3** could not be fully dissolved in neat MTBE, we have found that in the presence of vinyl butyrate the solubility of (±)-**3** was considerably enhanced, and thus the esterification process proceeded successfully, providing even better results when compared to a "classical" approach. It is important to mention that changing the synthetic strategy toward preparation of (±)-**4b** not only improved the reaction yield but also rendered a "greener" synthesis pathway by eliminating both the usage of methylene chloride as the solvent and the extraction procedure during the workup.

2.2. KR of (±)-3 Using Lipase-Catalyzed Transesterification—Lipase Selection. The development and optimization of a versatile enzymatic methodology are not simple and often lead to many laborious stages including the appropriate lipase selection, determining the effect of enzyme loading, pretreatment, and its conditioning as well as the adequate medium adjustment, proper choice of the acyl group type of donor/acceptor reagent, mutual substrate-to-biocatalyst-to-acyl group donor/acceptor molar/weight ratio, reaction time, temperature, etc. Rational planning of enzymatic reaction conditions is critical to meet sustainability criteria.

The water removal process is tedious and expensive at industrial scale. Hence, it is recommended to use synthetic approaches that allow the reactions to be carried out in pure easy-to-evaporate organic solvent or at least in an aqueous—organic two-phase system with the lowest possible water content. The realization of lipase-catalyzed (trans)esterification processes by means of an activated ester (e.g., enol esters, trifluoroethyl butyrate, *S*-ethyl thiooctanoate) seems to be the most suitable solution to overcome this problem. Therefore, at the outset of our study, the ability of lipases to catalyze the transesterification of proxyphylline (±)-**3** with an 11.5-fold molar excess of vinyl acetate as the acetyl transfer reagent in an anhydrous environment was investigated (Table 1). The enzymatic KR of the racemate (±)-**3** using excess vinyl acetate as the acetyl transfer reagent and the standard protocol was examined in chloroform since surprisingly only this solvent form homogeneous solution of the appropriate substrate concentration at 25 °C. None of the other tested solvents including those less polar than $CHCl_3$ [hexane, pentane, toluene, cyclohexane, 2-methyl-2-butanol (*tert*-amyl alcohol)] or more polar [diisopropyl ether, dichloromethane, MTBE, diethyl ether, vinyl acetate, tetrahydrofuran, acetone, acetonitrile, 1,4-dioxane] were suitable for enzymatic acetylation of (±)-**3**. Most of the reactions carried out in these solvents resulted in no substrate conversion mainly because of the low solubility of (±)-**3** in those media. Enzyme screening was attempted using a representative set of eight lipases isolated from various microorganisms including: *Candida antarctica B* (Novozym 435, Chirazyme L-2, c.-f., C2, Lyo., Chirazyme L-2, c.-f., C3, Lyo.), *Burkholderia cepacia* (Amano PS, Amano PS-IM), *Pseudomonas fluorescens* (Amano AK), *Thermomyces lanuginosus* (Lipozyme TL IM), and *Rhizomucor miehei* (Lipozyme RM IM).

Since the substrate (±)-**3** and product (±)-**4a** enantiomers do not separate on the available Chiralcel OD-H column, determination of the enantiomeric excess values directly from the crude reaction mixture over the course of the process was impossible. Therefore, the progress of the enzymatic reactions was at first traced by means of nonchiral gas chromatography (GC) with respect to the appropriate calibration curve for quantitative analyses. Next, the reactions were stopped as close to 50% substrate conversion as possible, subsequently isolation by column chromatography was performed, and only then the ee-values were determined by chiral HPLC. In addition, for determination of enantiopurity of title API an extra derivatization procedure of the alcohol into the corresponding acetate was required. For that reason, chemical protection of the remaining free hydroxyl functional group was performed by addition of acetic anhydride with a catalytic amount of DMAP in dry dichloromethane at room temperature, thus obtaining

DOI: 10.1021/acs.joc.5b01840
J. Org. Chem. 2016, 81, 380−395

Table 2. Lipase Screening for the Enantioselective Methanolysis of (±)-4a under Kinetically Controlled Conditions in CH_3CN

Entry	Lipase preparation[a]	t [d]	Conv. [%]	ee_s[b] [%]/(config.)	ee_p[c] [%]/(config.)	E[d]
1	Novozym 435	8	57[e]	95/(*S*)	72/(*R*)	22
2	Chirazyme L-2, C-2	8	53[e]	81/(*S*)	73/(*R*)	16
3	Chirazyme L-2, C-3	1	2[f]	N.D.[g]	N.D.[g]	N.D.[g]
4	Amano PS	1	0[f]	N.D.[g]	N.D.[g]	N.D.[g]
5	Amano PS-IM	1	0[f]	N.D.[g]	N.D.[g]	N.D.[g]
6	Amano AK	1	0[f]	N.D.[g]	N.D.[g]	N.D.[g]
7	Lipozyme TL IM	1	0[f]	N.D.[g]	N.D.[g]	N.D.[g]
8	Lipozyme RM IM	1	0[f]	N.D.[g]	N.D.[g]	N.D.[g]

[a]Conditions: (±)-**4a** 100 mg, lipase 20 mg, CH_3CN 1 mL, methanol 114 mg, 0.15 mL (10 equiv), 25 °C, 500 rpm (magnetic stirrer). [b]Determined by chiral HPLC analysis by using a Chiralcel OD-H column. [c]Determined by chiral HPLC analysis of corresponding alcohol obtained after derivatization of alcohol (*R*)-(−)-**3** into the corresponding acetate (*R*)-(−)-**4a**, which was performed by addition of DMAP and Ac_2O (5 equiv) since direct analysis of (*R*)-(−)-**3** with Chiralcel OD-H column was unsatisfactory. [d]Calculated according to Chen et al.,[42] using the equation: $E = \{\ln[(1-\text{conv.})(1-ee_s)]\}/\{\ln[(1-\text{conv.})(1+ee_s)]\}$. [e]Based on GC, for confirmation the % conversion was calculated from the enantiomeric excess of the unreacted ester (ee_s) and the product (ee_p) according to the formula conv. = $ee_s/(ee_s + ee_p)$. [f]Based on gas chromatography (GC). [g]Not determined.

optically active acetate (*S*)-(+)-**4a** or (*R*)-(−)-**4a** in quantitative yields from (*S*)-(+)-**3** or (*R*)-(−)-**3**, respectively.

Among the investigated panel of commercially available preparations, immobilized lipases of a fungal origin such as Novozym 435, Chirazyme L-2, C-2, and Chirazyme L-2, C-3 were established as the most potent biocatalysts for enantioselective transesterification. However, the lipase-catalyzed acetylation of (±)-**3** in $CHCl_3$ was not successful as the reaction rates and enantioselectivities (E = 2−9) were far from ideal. Moreover, the enantiomeric excesses of the desired products [(*S*)-(+)-**3** and (*R*)-(−)-**4a**] were low (18−76% ee), and in consequence, evaluation of an enzymatic transesterification of proxyphylline (±)-**3** approach was discontinued. The remaining lipases (Amano PS, Amano AK, Lipozyme RM IM) proved to be catalytically inactive even after 7 days of undergoing reaction, while Amano PS-IM and Lipozyme TL IM preparations showed poor selectivity.

2.3. KR of (±)-4a Using Lipase-Catalyzed Alcoholysis−Lipase Selection. Since it was impossible for acceptable reaction *E*-factors to comply with the *O*-acetylation procedure (Table 1), we have opted to use the reverse process, that is lipase-catalyzed alcoholysis of the acetate (±)-**4a** (Table 2). The enzymatic alcoholysis was conducted with methanol as an acetyl-acceptor reagent used in a relatively high ratio to the substrate (±)-**4a** (10 equiv) in spite of the well-known fact that most enzymes are inactivated by low-molecular-weight alcohols, particularly by methanol and ethanol. This stems from the propensity of polar/hydrophilic solvents to strip off the essential layer of water molecules from the protein (the structural water), thereby disrupting its native structure responsible for catalysis, and eventually denaturing the enzyme. However, this decision was made intentionally since we have observed the positive impact of methanol on the substrate (±)-**4a** solubility. Initially, the same panel of lipases (Table 1) was screened as catalysts of asymmetric methanolysis of racemic proxyphylline acetate (±)-**4a** at 25 °C. A detailed survey on the selection of the optimal lipase catalyst was carried out using acetonitrile as the solvent. Aliquots of the samples were withdrawn from the reaction mixture at 1 day intervals, and the samples were analyzed by GC. Next, the chromatographic purification and appropriate alcohol derivatization were performed, and the ee-values were measured by means of chiral HPLC. However, preliminary studies gave disappointing results. In most of the studied enzyme systems no reaction was observed (Table 2, entries 4−8) or the lipase-mediated KR proceeded sluggishly achieving barely 2% of the conversion after 24 h (Table 2, entry 3). Interestingly, Novozym 435 and Chirazyme L-2, C-2 catalyzed methanolysis of the acetate (±)-**4a**, showing promising selective enrichment of the products (Table 2, entries 1 and 2). However, the enantiomeric excess values of the liberated alcohol (*R*)-(−)-**3** (72−73% ee) as well as the reaction enantioselectivities (E = 16−22) in both cases were poor-to-moderate, and the requested 50% conversions were obtained after as much as 8 days. Although slightly better results in terms of enantioselectivity were obtained with the alcoholysis protocol compared to transesterification, still the process proceeded within an unreasonable time scale. In turn, as the results presented in Table 2 clearly indicate that (Novozym 435)-catalyzed methanolysis of (±)-**4a** yielded unreacted acetate (*S*)-(+)-**4a** with higher optical purity (95% ee) than Chirazyme L-2, C-2 (81% ee), we decided to assess immobilized CAL-B as a potential catalyst for further studies.

2.4. KR of (±)-4a Using Lipase-Catalyzed Alcoholysis − the Solvent Effect. Another important criterion when setting up an enzymatic catalysis with lipases for a given process is the choice of the reaction medium. Selection of an appropriate solvent system (so-called "medium engineering") for a particular enzyme−substrate pair is often a very laborious task, but if properly performed it can significantly improve the activity, stability, and selectivity of the biocatalyst and additionally may even influence the stereochemical preference of the biocatalyst.[43]

This stage of our study has been aimed to optimize the (Novozym 435)-catalyzed KR in the alcoholysis of (±)-**4a** with methanol mainly by assessment of the influence of solvent on the conversion rate and stereochemical outcome. For this purpose, alternative "green solvents" (CH_3CN, 1,4-dioxane, and acetone), traditional organic solvents with low eco-toxicity ($PhCH_3$, THF), and undesirable chlorinated solvents ($CHCl_3$, CH_2Cl_2) were examined as the reaction media. In other commonly used solvents, well-known for their compatibility with lipases, such as MTBE, diisopropyl ether (DIPE), *n*-hexane, and 2-methylbutan-2-ol (*tert*-amyl alcohol, TAA), most of the acetate (±)-**4a** remained in suspension due to poor solubility, and therefore for obvious reasons the reactions were not performed. A screen of media showed that this method also failed to give high enantioselectivities, as the best results were

DOI: 10.1021/acs.joc.5b01840
J. Org. Chem. 2016, 81, 380−395

obtained still with Novozym 435 suspended in CH_3CN. However, a few observations are noteworthy. Despite the common rule that in lipase-catalyzed reactions hydrophobic solvents provide a higher reaction rate than hydrophilic ones, in our investigations we observed the opposite tendency. This is a surprising result because Novozym 435 was found to retain its catalytic potency in the polar solvents (Table 3, entries 1–3), showing very similar enantioselectivities (E = 20–23), while in most of the employed less polar solvents it was inactive toward (±)-**4a** (Table 3, entries 4–6). However, the last result (Table 3, entry 4) indicates that the activity of the lipases might be affected by the solvent without correlation to log P, and therefore other parameters such as solvent–enzyme–substrate interactions cannot be ignored; i.e. the accessibility of the substrate to the enzyme active site might be induced by diffusional limitations, changes in protein flexibility, or some allosteric regulation controlled by the solvent. Although the reaction was conducted in toluene, unreacted acetate (*S*)-(+)-**4a** was obtained with a high 92% ee; however, both the reaction rate and the enantioselectivity were very low indeed. Notably, when comparing both types of the studied lipase-catalyzed reactions, one can see some characteristic behavior. It turned out that (Novozym 435)-catalyzed transesterification of (±)-**3** in chloroform proceeded quite successfully; nevertheless, in the case of methanolysis of (±)-**4a**, the activity of this enzyme was completely lost in water-immiscible chlorinated cosolvents ($CHCl_3$ or CH_2Cl_2), as the process did not start even after a day. Finally, acetonitrile was found to be the solvent of choice for lipase-mediated methanolysis of (±)-**4a**, where other solvents offered decreased rates and worse enantioselectivities.

Table 3. Solvent Screening for the Enantioselective Methanolysis of (±)-4a in the Presence of Novozym 435 under Kinetically Controlled Conditions

Entry	Solvent[a] (log P)[b]	t [d]	Conv. [%]	ee_s[c] [%]/(config.)	ee_p[d] [%]/(config.)	E[e]
1	1,4-Dioxane (−0.31)	10	60[f]	97/(*S*)	66/(*R*)	20
2	CH_3CN (0.17)	8	57[f]	95/(*S*)	73/(*R*)	23
3	Acetone (0.20)	10	54[f]	89/(*S*)	75/(*R*)	21
4	THF (0.40)	1	0[g]	N.D.[h]	N.D.[h]	N.D.[h]
5	$CHCl_3$ (1.67)	1	0[g]	N.D.[h]	N.D.[h]	N.D.[h]
6	CH_2Cl_2 (1.01)	1	0[g]	N.D.[h]	N.D.[h]	N.D.[h]
7	$PhCH_3$ (2.52)	14	63[f]	92/(*S*)	54/(*R*)	10

[a]Conditions: (±)-**4a** 100 mg, lipase 20 mg, solvent 1 mL, methanol 114 mg, 0.15 mL (10 equiv), 25 °C, 500 rpm (magnetic stirrer). [b]Logarithm of the partition coefficient of a given solvent in *n*-octanol–water system according to ChemBioDraw Ultra 13.0 software indications. [c]Determined by chiral HPLC analysis by using a Chiralcel OD-H column. [d]Determined by chiral HPLC analysis of corresponding alcohol obtained after derivatization of alcohol (*R*)-(−)-**3** into the corresponding acetate (*R*)-(−)-**4a**, which was performed by addition of DMAP and Ac_2O (5 equiv) since direct analysis of (*R*)-(−)-**3** with Chiralcel OD-H column was unsatisfactory. [e]Calculated according to Chen et al.,[42] using the equation: $E = \{\ln[(1 - \text{conv.})(1 - ee_s)]\}/\{\ln[(1 - \text{conv.})(1 + ee_s)]\}$. [f]Based on GC, for confirmation the % conversion was calculated from the enantiomeric excess of the unreacted ester (ee_s) and the product (ee_p) according to the formula conv. = $ee_s/(ee_s + ee_p)$. [g]Based on gas chromatography (GC). [h]Not determined.

2.5. Lipase-Catalyzed KR of (±)-4a–b – Alcoholysis vs Hydrolysis. Adverse results of (±)-**4a** kinetic resolution forced us to explore an alternative asymmetric approach toward the synthesis of optically active proxyphylline. In living organisms, lipases catalyze hydrolysis of higher fatty acid esters of glycerol, thus fulfilling an essential function in the metabolism of lipids (e.g., fats and oils) and lipoproteins. As lipases are natural "workhorses" of such chemical transformations in the cells, it seems reasonable to increase the lipophilicity of proxyphylline (±)-**3** by replacing the acetate moiety with longer fatty acyl chains. We envisaged that by using butyrate (±)-**4b** or decanoate (±)-**4c** derivatives, which mimc closer natural substrates, the reactions might occur with enhanced enantioselectivity. Unfortunately, monitoring of the enzymatic reaction with proxyphylline decanoate (±)-**4c** was impossible since GC and HPLC analyses both failed due to the nonvolatility of

Table 4. Examination of (Novozym 435)-Catalyzed KR Conditions for the Enantioselective Methanolysis and Hydrolysis of (±)-4a and (±)-4b Suspended in CH_3CN after 8 Days, respectively

Entry	Compound	Nucleophile	Conv.[a] [%]	ee_s[b] [%]/(config.)	ee_p[c] [%]/(config.)	E[d]
1	(±)-**4a**	MeOH[e]	57	95/(*S*)	73/(*R*)	23
2		H_2O[f]	41	64/(*S*)	94/(*R*)	63
3		Tris-HCl Buffer[g]	62	52/(*S*)	84/(*R*)	8
4	(±)-**4b**	MeOH[h]	57	>99/(*S*)	74/(*R*)	34
5		H_2O[i]	51	98/(*S*)	94/(*R*)	149
6		Tris-HCl Buffer[j]	50	96/(*S*)	97/(*R*)	260

[a]Based on GC, for confirmation the % conversion was calculated from the enantiomeric excess of the unreacted ester (ee_s) and the product (ee_p) according to the formula conv. = $ee_s/(ee_s + ee_p)$. [b]Determined by chiral HPLC analysis by using a Chiralcel OD-H column. [c]Determined by chiral HPLC analysis of corresponding alcohol obtained after derivatization of alcohol (*R*)-(−)-**3** into the corresponding acetate (*R*)-(−)-**4a**, which was performed by addition of DMAP and Ac_2O (5 equiv) since direct analysis of (*R*)-(−)-**3** with Chiralcel OD-H column was unsatisfactory. [d]Calculated according to Chen et al.,[42] using the equation: $E = \{\ln[(1 - \text{conv.})(1 - ee_s)]\}/\{\ln[(1 - \text{conv.})(1 + ee_s)]\}$. [e]Conditions: (±)-**4a** 100 mg, lipase 20 mg, CH_3CN 1 mL, MeOH 114 mg, 0.15 mL (10 equiv), 25 °C, 500 rpm (magnetic stirrer). [f]Conditions: (±)-**4a** 100 mg, lipase 20 mg, CH_3CN 1 mL, H_2O 64 mg, 0.64 mL (10 equiv), 25 °C, 500 rpm (magnetic stirrer). [g]Conditions: (±)-**4a** 100 mg, lipase 20 mg, CH_3CN 1 mL, 1 M Tris-HCl Buffer, pH 7.5 64 mg, 0.64 mL (10 equiv), 25 °C, 500 rpm (magnetic stirrer). [h]Conditions: (±)-**4b** 100 mg, lipase 20 mg, CH_3CN 1 mL, MeOH 104 mg, 0.13 mL (10 equiv), 25 °C, 500 rpm (magnetic stirrer). [i]Conditions: (±)-**4b** 100 mg, lipase 20 mg, CH_3CN 1 mL, H_2O 58 mg, 0.58 mL (10 equiv), 25 °C, 500 rpm (magnetic stirrer). [j]Conditions: (±)-**4b** 100 mg, lipase 20 mg, CH_3CN 1 mL, 1 M Tris-HCl Buffer, pH 7.5 58 mg, 0.58 mL (10 equiv), 25 °C, 500 rpm (magnetic stirrer).

DOI: 10.1021/acs.joc.5b01840
J. Org. Chem. 2016, 81, 380–395

(±)-**4c** within the recommended temperature range limits (<260 °C) for the available HP-50+ semipolar column and the nonresolvability of (±)-**4c** enantiomers on a Chiralcel OD-H column, respectively. These led us to cease further experiments with (±)-**4c**, and hence, we focused on the alcoholysis of acetate (±)-**4a** and butanoate (±)-**4b**. Additionally, the enzymatic KR was examined in water-miscible (monophasic aqueous−organic) solvent systems composed of acetonitrile and water or commercially available 1 M Tris-HCl buffer, respectively (Table 4). The influence of the acyl group on the course of the ester methanolysis/hydrolysis reaction was examined using 10 equiv of the appropriate acyl acceptor reagent (methanol, H_2O or water which is present in buffer solution) under catalysis of Novozym 435 suspended in CH_3CN as cosolvent, with stirring at 25 °C using a magnetic stirrer (500 rpm). The courses of all the enzymatic reactions were monitored by gas chromatography (GC), arrested deliberately after 8 days; all of the lipase-catalytically resolved products were chromatographically purified, the hydroxyl group of (*R*)-(−)-**3** was properly derivatized, and only then their final evolutions were subsequently followed by chiral HPLC to compare the efficiency of the particular methodology. At first glance, the size of the acyl group in the examined esters (±)-**4a**−**b** strongly influences the reaction enantioselectivity. The results presented in Table 4 indicate that KR of butanoate (±)-**4b** proceeded with a considerable improvement in the reaction enantioselectivity (*E* up to 260), furnishing in the case of both types of hydrolytic attempts (Table 4, entry 5 and 6) very good results in terms of the enantiomeric excess of unreacted ester (*S*)-(+)-**4b** (96−98% ee) as well as the released alcohol (*R*)-(−)-**3** (94−97% ee). In turn, although (Novozym 435)-catalyzed methanolysis of (±)-**4b** was significantly less selective (*E* = 34), it turned out that enantioenrichment was remarkably high as the ester (*S*)-(+)-**4b** was obtained with an excellent enantiomeric excess (>99% ee). Moreover, a comprehensive understanding of the kinetics of lipase-catalyzed reactions prompts us to consider that the potential of methanolysis of (±)-**4b** has not been fully evaluated, and an attractive optical purity could be obtained for the opposite enantiomer (*R*)-(−)-**3** as well. This is fully understandable especially since one realizes that Chen's logarithmic equation[42] demands very similar levels of conversion, so that the the *E*-factor results may be reliably compared. As a single experiment cannot be decisive for the full estimation of enzymatic performance as well as its potential applicability, it was therefore desirable to compare two types of lipase-mediated transformations: hydrolysis of (±)-**4b** in Tris-HCl buffer as the most enantioselective method, and methanolysis of (±)-**4b** as the one which led to the highest enantiomeric excess of unreacted ester (*S*)-(+)-**4b**.

Stimulated by the above-mentioned results, in the next part of our study, we examined the time dependency on the rate and enantioselectivity of butyrate (±)-**4b** methanolysis/hydrolysis under kinetic resolution conditions described in the previous section. For that reason, the conversion degrees of enzymatic reactions were monitored by chiral HPLC over a wide range of reaction times and at various intervals. From the data collected in Table 5 it became obvious that the methanolysis reaction proceeded more enantioselectively (up to *E* = 584) to give both unreacted substrate (*S*)-(+)-**4b** and product (*R*)-(−)-**3** in enantiomerically pure form (>99% ee) depending on the moment of process arresting. Another clear advantage of lipase-catalyzed methanolysis over the hydrolysis method is the ease of methanol removal by evaporation under reduced pressure or by extraction, so there is no need to use special water removal procedures.

Table 5. Examination of (Novozym 435)-Catalyzed KR Time Courses for the Enantioselective Methanolysis and Hydrolysis of (±)-4b Suspended in CH_3CN, Respectively

Entry	Nucleophile	*t* [h]	Conv.[a] [%]	ee_s[b] [%]/(config.)	ee_p[c] [%]/(config.)	*E*[d]
1	MeOH[e]	4	46	84/(*S*)	>99/(*R*)	532
2		8	47	88/(*S*)	>99/(*R*)	584
3		24	48	90/(*S*)	96/(*R*)	152
4		48	52	>99/(*S*)	92/(*R*)	126
5		72	52	>99/(*S*)	90/(*R*)	99
6		96	53	>99/(*S*)	88/(*R*)	82
7	Tris-HCl Buffer[f]	24	30	43/(*S*)	98/(*R*)	151
8		48	39	63/(*S*)	98/(*R*)	190
9		72	45	80/(*S*)	98/(*R*)	244
10		96	46	84/(*S*)	98/(*R*)	264
11		120	46	85/(*S*)	98/(*R*)	270
12		144	47	87/(*S*)	98/(*R*)	283

[a]Based on GC, for confirmation the % conversion was calculated from the enantiomeric excess of the unreacted ester (ee_s) and the product (ee_p) according to the formula conv. = $ee_s/(ee_s + ee_p)$. [b]Determined by chiral HPLC analysis by using a Chiralcel OD-H column. [c]Determined by chiral HPLC analysis of corresponding alcohol obtained after derivatization of alcohol (*R*)-(−)-**3** into the corresponding acetate (*R*)-(−)-**4a**, which was performed by addition of DMAP and Ac_2O (5 equiv) since direct analysis of (*R*)-(−)-**3** with Chiralcel OD-H column was unsatisfactory. [d]Calculated according to Chen et al.,[42] using the equation: $E = \{\ln[(1-conv.)(1-ee_s)]\}/\{\ln[(1-conv.)(1+ee_s)]\}$. [e]Conditions: (±)-**4b** 100 mg, lipase 20 mg, CH_3CN 1 mL, MeOH 104 mg, 0.13 mL (10 equiv), 25 °C, 500 rpm (magnetic stirrer). [f]Conditions: (±)-**4b** 100 mg, lipase 20 mg, CH_3CN 1 mL, 1 M Tris-HCl Buffer, pH 7.5 58 mg, 0.58 mL (10 equiv), 25 °C, 500 rpm (magnetic stirrer).

Analysis of data from kinetic experiments also highlighted how the reaction rates differ substantially in each case. It was observed that the rate of (Novozym 435)-mediated methanolysis of (±)-**4b** was profoundly enhanced compared to hydrolysis, as it reaches ca. 50% conversion after approximately 24 h, while hydrolysis catalyzed by the same lipase could not achieve this level even after elongation of the reaction time over 6 days. By comparing both enantioselective KR courses, one can note the very characteristic tendency. Although the hydrolytic attempt excludes the possibility of achieving enantiopure alcohol (*R*)-(−)-**3** during the examined time period, the liberated alcohol has always been afforded with excellent enantiomeric excesses of about 98% (Table 5, entries 7−12). In turn, an enantioenrichment increment of the slower reacting enantiomer (*S*)-(+)-**4b** was negligible, and it finally reached barely 87% ee. In the case of enantioselective hydrolysis of (±)-**4b** it was observed that the conversion increased to a certain level (45−47%) after which there was no significant change (Table 5, entries 9−12). Note also that it was crucial to follow the kinetics of both lipase-catalyzed reactions very carefully, as it allowed us to determine the appropriate moment to terminate the biotransformation of (±)-**4b** in order to obtain products of desired enantiomeric purity. Undoubtedly, the experiments revealed the classic kinetics of the process that means when the lipase-mediated methanolysis process does not exceed 47% conversion, it is in favor of enantiopure

DOI: 10.1021/acs.joc.5b01840
J. Org. Chem. 2016, 81, 380−395

Table 6. Gram- and Multigram-Scale Enantioselective Methanolysis of (±)-4b Catalyzed by Novozym 435

Entry	Scale	t [d]	Conv.[a] [%]	ee_s[b] [%]/Yield[e] (%)/$[\alpha]_D$[f]	ee_p[c] [%]/Yield[e] (%)/$[\alpha]_D$[f]	E[d]
1	1 g[g]	1	47	87/95/+42.96 (c 1.35)	98/89/−54.00 (c 1. 00)	283
2		3	51	>99/96/+50.36 (c 1.40)	94/90/−50.00 (c 1.00)	170
3	2 g[h]	1	48	88/93/+36.00 (c 1.50)	97/93/−52.38 (c 1.05)	192
4		3	51	>99/94/+45.29 (c 1.70)	95/89/−51.43 (c 1.05)	206
5	5 g[i]	2	50	97/90/+41.35 (c 1.85)	96/91/−48.00 (c 1.05)	207
6		6	53	>99/93/+48.89 (c 1.80)	89/94/−47.14 (c 1.00)	90

[a]Based on GC, for confirmation the % conversion was calculated from the enantiomeric excess of the unreacted ester (ee_s) and the product (ee_p) according to the formula conv. = $ee_s/(ee_s + ee_p)$. [b]Determined by chiral HPLC analysis by using a Chiralcel OD-H column. [c]Determined by chiral HPLC analysis of corresponding alcohol obtained after derivatization of alcohol (*R*)-(−)-**3** into the corresponding acetate (*R*)-(−)-**4a**, which was performed by addition of DMAP and Ac_2O (5 equiv) since direct analysis of (*R*)-(−)-**3** with Chiralcel OD-H column was unsatisfactory. [d]Calculated according to Chen et al.,[42] using the equation: $E = \{\ln[(1 - \text{conv.})(1 - ee_s)]\}/\{\ln[(1 - \text{conv.})(1 + ee_s)]\}$. [e]This value indicates isolated yield after purification step and is calculated on the basis of the theoretical number of moles arising from conversion rate, relative to theoretical amount; i.e., when 50% conversion is reached, up to the half of the acetate could be obtained. [f]Specific rotation, c solution in chloroform, T = 27.5 °C. [g]Conditions: (±)-**4b** 1 g, lipase 200 mg, CH_3CN 10 mL, MeOH 1.04 g, 1.3 mL (10 equiv), 25 °C, 500 rpm (magnetic stirrer). [h]Conditions: (±)-**4b** 2 g, lipase 400 mg, CH_3CN 20 mL, MeOH 2.08 g, 2.6 mL (10 equiv), 25 °C, 500 rpm (magnetic stirrer). [i]Conditions: (±)-**4b** 5 g, lipase 1 g, CH_3CN 50 mL, MeOH 5.20 g, 6.6 mL (10 equiv), 25 °C, 500 rpm (magnetic stirrer).

alcohol (*R*)-(−)-**3** formation (Table 5, entries 1 and 2), while when reaching a conversion above 52% (Table 5, entries 4−6), it is beneficial for obtaining unreacted ester (*S*)-(+)-**4b** as a single enantiomer (>99%). It is noteworthy that the maximum enantiomeric excesses of the product (92%) and substrate (>99%) from the same attempt were obtained when the reaction was arrested at a conversion of ca. 52% after 2 days (Table 5, entry 4).

2.6. Preparative-Scale Lipase-Catalyzed KR of (±)-4b via Methanolysis. Gratifyingly, an in-depth analysis performed on biotransformation reaction conditions allowed us to obtain a strategy that is fully compatible for the employed xanthine-like derivative (±)-**4b**. In the course of our investigation, we found that enzyme-promoted methanolysis unequivocally was the method of choice, as it led to both resolved enantiomers of proxyphylline in high enantiomeric purity, depending on the time and conversion rate. As we developed a reliable and robust catalytic system at analytical scale, next we focused on the lipase-catalyzed methanolysis of (±)-**4b** under the conditions of kinetic resolution at preparative scale. The commercial CAL-B in immobilized form (Novozym 435) was employed as the catalyst. A crucial advantage of the above-selected lipase preparation is its ease of handling and simple isolation of the resolved products. The up-scaling investigations were carried out with 1, 2, and 5 g of butanoate (±)-**4b** respectively using the same optimized reaction procedure as in the analytical scale studies, but obviously with proportionally enlarged reaction stoichiometry (Table 6). Unfortunately, we have found that when performing enzymatic processes on a larger scale, different reaction times were required to obtain both enantiomers of proxyphylline with comparable % ee. The reason for such behavior is unclear to us because we have not met any drawbacks in up-scaling to this point. This suggests that the discrepancy mostly appears at the process monitoring stage. As we mentioned earlier, during this synthesis we could not optimize the HPLC analytic method for reliable tracing of the reaction progress directly from the crude mixture. In this instance, the differences in experimental attempts may be due to the GC analysis used, which is definitely saddled with some error and might appear to be the main source of inaccuracies. Nevertheless, from the results summarized in Table 6, it is evident that preparative scale methanolysis of (±)-**4b** provided access to both enantiomers of proxyphilline reaching a very high (94−97% ee) to excellent enantiomeric enrichment (98−100% ee).

In response to 1 g reactions, Novozym 435 exhibited excellent enantioselection (E = 170−283) in the preparative methanolysis of substrate (±)-**4b** providing access to the ester (*S*)-(+)-**4b** with >99% ee and to alcohol (*R*)-(−)-**3** with 98% ee (Table 6, entries 1 and 2) depending on the time of the process termination and thus the conversion. In the case of 2 g scale reactions one can see that the results strongly correlated with the previous 1 g scale attempts (Table 6, entries 1 and 2 vs entries 3 and 4). Hence, if the reaction was arrested after 24 h of processing, Novozym 435 acted with a high stereopreference in the formation of alcohol (*R*)-(−)-**3** (97% ee) (Table 6, entry 3), whereas the reaction terminated after 3 days yielded unreacted ester (*S*)-(+)-**4b** with >99% ee (Table 6, entry 4). Finally we scaled-up the reaction to 5 g of racemic substrate (±)-**4b** reaching similar ee values to those presented, but after twice as long reaction times. The lower reaction rate might be due to the lower level of enzyme activity regarding the mass transfer coefficient, which in this case mostly depends on the relevant type of the employed reactor. To reach higher conversions in shorter reaction times, the amount of lipase should be doubled and/or the biotransformation of (±)-**4b** carried out at higher temperatures. However, the industry sector prefers simple reaction systems in which enzyme loading does not exceed 20% (w/w) in relation to substrate due to cost-effectiveness, and elevated temperatures are not willingly applied because of solvent volatility problems, a decrease in lipase stereopreference, and limitations in catalyst reusability. As the preparative scale reactions allowed us to obtain enantiomerically pure ester (*S*)-(+)-**4b** (>99% ee) for acceptable kinetics and showed potential in being amenable to a large-scale execution, the effects of enzyme concentration and temperature on the activity and enantioselectivity of Novozym 435 for the KR of (±)-**4b** were intentionally not studied. Examination of the data included in Table 6 reveals that scaling of the reaction up to 1, 2, and, subsequently, up to 5 g of the substrate (±)-**4b** gave almost the same isolated yields of recovered ester (*S*)-(+)-**4b** ranging from 90% to 96%, and the formed alcohol (*R*)-(−)-**3** ranging from 89% to 93% with high to excellent enantiomeric excess (87−100% ee) for both resolved enantiomers. In addition, the reusability of the biocatalyst was tested by conducting the same experiments with the spent catalyst, and we found that Novozym 435 did

DOI: 10.1021/acs.joc.5b01840
J. Org. Chem. 2016, 81, 380−395

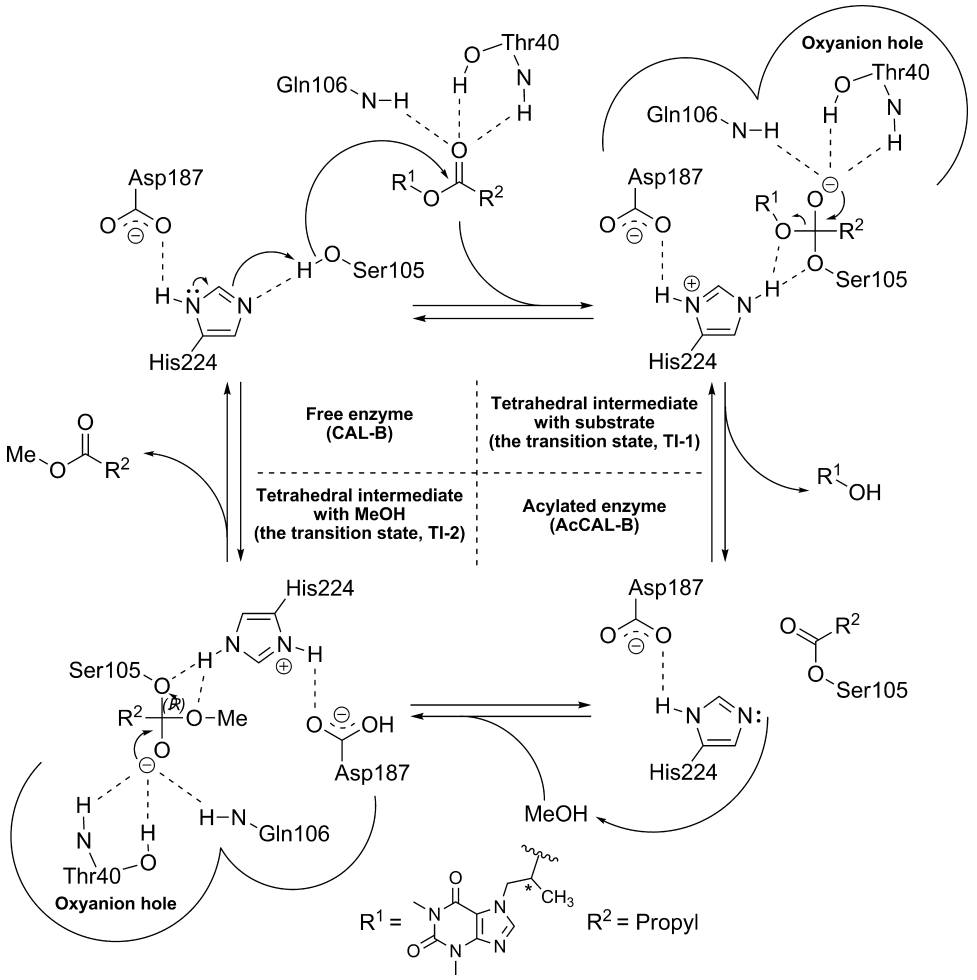

Figure 1. Reaction mechanism (catalytic cycle) of the (CAL-B)-catalyzed methanolysis of (±)-**4b**.

not show any significant activity loss and erosion of ee even after three reuses. This can be recognized as a crucial advantage, since the lipase experienced prolonged contact with the stirring bar, which can mechanically crush the immobilization support, resulting in detachment of the enzyme from the carrier, as well as contact with methanol during the reaction, and with chloroform while the filtration and washing procedures were performed. Interestingly, we have found that the resultant alcohol (*R*)-(−)-**3** was precipitated as a crystalline solid during the progress of the reaction. The phenomenon of selective solubility of the alcohol and butanoate in the chosen medium (CH_3CN) potentially increases the utility and practical application of the used synthetic route, as the cumbersome chromatography purification step might be fully excluded after the KR procedure. This can be successfully used in both liquid−liquid extractive membrane reactors and/or immobilized enzyme biocatalytic membrane reactors (BMRs) commonly used in industry. The experimental validity of this feature will be verified more deeply in our laboratory in due course by conducting enzymatic reactions on a larger scale.

2.7. Determination of the Lipase Stereopreference. Lastly, the absolute configurations of both separated enantiomers [(*S*)-(+)-**4b** and (*R*)-(−)-**3**] were determined by comparison of their optical rotation signs with the data described in the literature. The optical rotation measured for samples of enantiomerically pure butyric ester (*S*)-(+)-**4b** (>99% ee) obtained by us varied from $[\alpha]_D^{27.5}$ = +45.29 (*c* 1.70, $CHCl_3$) to $[\alpha]_D^{27.5}$ = +50.36 (*c* 1.40, $CHCl_3$) depending on the source of their origin (experiment). In turn, the optical rotation determined for the most enantiomerically enriched alcohol (*R*)-(−)-**3** gave $[\alpha]_D^{27.5}$ = −54.00 (*c* 1.00, $CHCl_3$) at 98% ee, which is in accordance with the value given in literature $[\alpha]_D^{20}$ = −63.80 (*c* 0.42, $CHCl_3$) at >99% ee for the compound obtained from enantiomerically pure propylene oxide under basic conditions.[39] In light of these findings it is clear that the employed Novozym 435 exhibits (*R*)-stereopreference toward racemic ester (±)-**4b**, since in all of the attempted enzymatic assays it predominantly catalyzed the transformation of the (*R*)-enantiomer into the corresponding optically active alcohol (*R*)-(−)-**3** leaving the (*S*)-ester almost unreacted. It is reasonable to assume that Novozym 435 manifests the same enantiopreference with (±)-**3** in transesterification reactions, giving the complementary results to lipase-mediated methanolysis in terms of stereochemistry of the resolved enantiomers.

2.8. Docking. There is clearly an urgent need for development of more effective strategies for synthetic methods; hence, in-depth knowledge of the catalytic behavior of the enzymes as natural asymmetric selectors toward chiral molecules is beneficial. Limited attention has been devoted so far to gaining a deeper understanding of the molecular basis of the lipase-catalyzed processes.[44] Therefore, employment of molecular modeling techniques using docking tools, molecular dynamics (MD) procedures, and quantum mechanics/molecular mechanics (QM/MM) calculations to gain insight into the

DOI: 10.1021/acs.joc.5b01840
J. Org. Chem. 2016, 81, 380−395

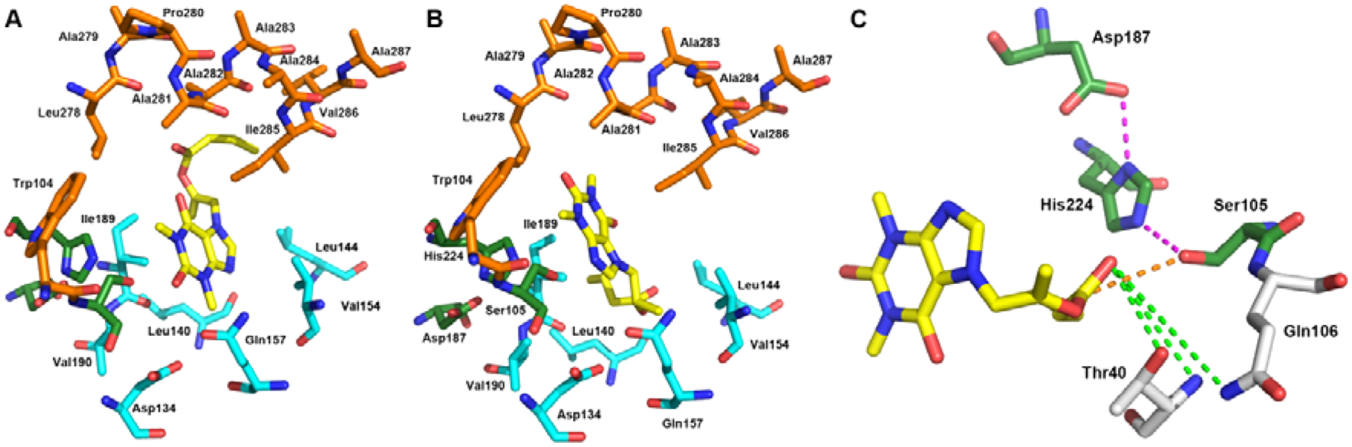

Figure 2. Characteristic binding modes of racemic proxyphylline butanoate (±)-**4b** (yellow sticks) in the CAL-B (PDB ID: 1TCA) binding pocket. The active-site geometries of CAL-B with (±)-**4b** docked in binding mode I (A) and in binding mode II (B). The binding pocket of CAL-B is constituted by a medium hydrophobic pocket (orange sticks) above the catalytic triad Asp-His-Ser (green sticks) and a large pocket (cyan sticks) below it (A and B). (C) The most important interatomic distances for the catalytic process between substrate (±)-**4b**, catalytic triad, and the oxyanion hole residues (gray sticks) of the CAL-B are indicated by magenta, green, and orange dashed lines, respectively. The figures were generated using PyMOL.

mechanistic details of lipase catalytic properties should allow rational design of substrates (substrate engineering), reaction conditions (medium engineering), and enzymes (protein engineering) for improved reaction kinetics, yields, and higher enantioselectivity.

In order to rationalize the observed enantioselectivity of the (CAL-B)-catalyzed methanolysis of (±)-**4b**, we applied an enzyme−substrate docking protocol using noncommercial AutoDock Vina software.[45] According to the well-known mechanism of action of serine hydrolases,[46] the employed immobilized CAL-B (Novozym 435) catalyzes the methanolysis of (±)-**4b** in the manner depicted in Figure 1. In general, the CAL-B active site consists of a catalytic triad of Ser105, His224, and Asp187 in which serine is the key amino acid engaged in biotransformations of xenobiotic substrates, and the remaining two residues are responsible for its nucleophilic activation. The mechanism of the (CAL-B)-catalyzed methanolysis of racemic butanoate (±)-**4b** involves two steps during which two noncovalent enzyme−substrate complexes [namely, Michaelis complexes (MCCs)] and tetrahedral intermediates (TIs) are formed. In the first step of the reaction, the activated nucleophilic hydroxyl group of the Ser105 attacks the acyl-carbonyl group of the substrate (±)-**4b**, thus affording the acyl-enzyme intermediate (acylation step). The formation and collapse of the first tetrahedral intermediate (TI-1) is the rate-determining step of a whole catalytic process. In the second step, the acyl group of the acylated enzyme (AcCAL-B) reacts with nucleophilic methanol (deacylation step) to form the second tetrahedral intermediate (TI-2), and finally to liberate the enzyme closing the catalytic cycle. In addition, both TIs are stabilized by NH and OH functions in the so-called oxyanion hole of the enzyme, constituted by the Gln106 and Thr40 residues (see Figure 1).

Moreover, the binding side of CAL-B is composed of two hydrophobic pockets: the large pocket is lined by the respective set of Ile189, Val190, Val154, Leu140, Leu144, Asp134, and Gln157 residues, while the medium pocket is crowded by Trp104 and the Leu278−Ala287 helix. The architecture of these pockets force substrate (±)-**4b** to accommodate within the active site of CAL-B in two binding modes, namely binding mode I (Figure 2 A) and binding mode II (Figure 2 B), thereby determining the orientation of the substrate molecule toward the catalytic triad and the oxyanion hole residues. Because some part of more bulky substrates may extend toward the entrance of the medium-size hydrophobic pocket, the interactions with the solvent in the particular binding mode is obviously relevant as well. For the formation of the enzyme−substrate active complex, the proper location of the substrate acyl group against the hydroxyl group of the catalytic Ser105 as well as the appropriate interatomic distances, including the catalytic intramolecular hydrogen bonding network between Asp187 and His224 residues, which lead to abstraction of an acidic proton from the hydroxyl group of Ser105, and thus facilitate the nucleophilic attack (Figure 2 C magenta dashes), must be maintained. Bearing in mind all of the above-mentioned requirements, we have taken into account three major criteria when employing docking studies: (i) the distance of the carbon atom of the carbonyl group of the alkyl side chain of (±)-**4b** to the oxygen atom of the OH group of the catalytic serine (Figure 2 C orange dashes), (ii) hydrogen bond interactions between the acetyl oxygen of (±)-**4b** and the residues of the oxyanion hole (Figure 2 C green dashes), (iii) steric clashes with the enzyme, and (iv) other intermolecular polar interactions.

To disclose the structural factors responsible for the higher reactivity of the (*R*)-ester than its counterpart in the lipase-catalyzed methanolysis reactions of (±)-**4b**, the two enantiomers of proxyphylline butanoate [(*S*)-(+)-**4b** and (*R*)-(−)-**4b**] were docked separately in the CAL-B structure taken from the Protein Data Bank (PDB), with the code 1TCA.[47] Before docking was performed, the target structure of CAL-B was appropriately prepared by deleting all the water molecules (including those that were present in the catalytic cavity) and by adding polar hydrogen atoms (see Experimental Section). When both enantiomers of (±)-**4b** were docked independently into the CAL-B active site, nine of the most energetically favorable binding modes for the ligand-protein complexes for each substrate molecule were generated. The results of binding affinity energies (kcal/mol) of the two ligands with the CAL-B enzyme are shown in Tables S2 and S3, which are placed in the

DOI: 10.1021/acs.joc.5b01840
J. Org. Chem. 2016, 81, 380−395

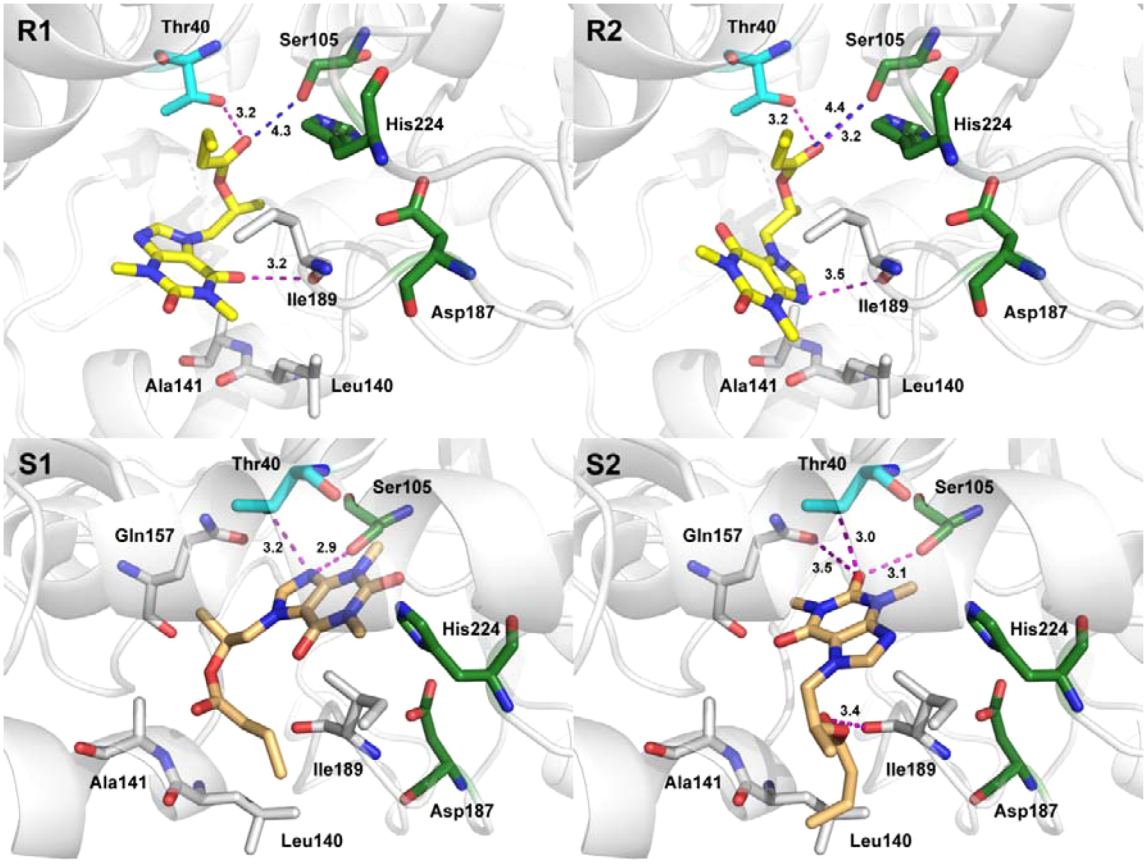

Figure 3. Predominant conformations of (*R*)-(−)-**4b** (yellow sticks) (R1−R2) and (*S*)-(+)-**4b** (lightorange sticks) (S1−S2) in CAL-B (PDB ID: 1TCA) active site. The residues constituting the catalytic triad (Asp187-His224-Ser105) of CAL-B are shown in green sticks representation. The oxyanionic Thr40 residue is shown in cyan. The rest of the most significant residues contributing to the stabilization of (±)-**4b** enantiomers by polar interactions (magenta dashed lines) and by CH−CH van der Waals (vdW) interactions are shown in gray sticks representation. Nitrogen atoms are presented with blue color, and the oxygen atoms with red color. The overall enzyme structure is shown as a gray cartoon diagram. The mutual distances between the amino acid residues, and ligands atoms are given in Ångström. The different orientation of the enantiomers toward Ser105 and Thr40 is clearly visible. Only the fast-reacting (*R*)-enantiomer (R1 and R2) is near Ser105 (4.3−4.4 Å; the distances are indicated by blue dashed lines) and additionally stabilized through the formation of hydrogen bonds (magenta dashes) with the Thr40 residue (3.2 Å) and Ile189 (3.2−3.5 Å).

Supporting Information. The next step provided a detailed analysis of all the unproductive and productive poses (a stable conformations that enable the generation of an acyl-enzyme reactive complexes) selected on the basis of the docking conformational search.

Concerning the two examined enantiomers of substrate (±)-**4b**, it was clear that only the *R*-enantiomer displayed a consistent orientation within the CAL-B binding site to obtain near attack conformations (NACs) leading to productive complexes (R1 and R2). As shown in Figure 3, the fast-reacting (*R*)-enantiomer is embraced inside the hydrophilic pockets of CAL-B in a position corresponding to the binding mode II postulated above (see Figure 2 B). In this case, the large substituent (1,3-dimethylxanthine group) was oriented toward the active-site entrance surrounded by hydrophobic Val154, Leu144, Ala141, Leu140, and Ile189 residues; meanwhile, the acyl moiety was positioned in the stereospecificity acid-binding pocket surrounded by Trp104 and Gln157. All the hydrogen bonds required for catalysis were spatially arranged, and the distance between the Ser105 residue and the carbonyl function of the (*R*)-ester was suitable for effective nucleophilic attack. Nevertheless, the selected docking conformations of the (*R*)-enantiomer (R1 and R2) illustrated in Figure 3 are not optimal for lipase catalysis, as the distances between the carbonyl atom in the acyl moiety and the oxygen atom of the catalytic serine exceed >4 Å (blue dashed lines), and it is too far for rapid nucleophilic attack to occur. Importantly, this can explain the slow lipase-mediated reaction of the employed racemic substrate (±)-**4b**. Moreover, the productive conformers of the fast-reacting enantiomer are efficiently stabilized by polar interactions (magenta dashed lines) between the carbonyl oxygen atom of (*R*)-ester and the oxyanion hole Thr40 residue as well as the hydrogen bonds formed between the carboxylic group of Ile189 and the oxygen atom (R1) or nitrogen atom (R2) of xanthine ring, respectively.

In sharp contrast to the (*R*)-ester, all the complexes of the slow-reacting (*S*)-enantiomer remains at the outer region of the active site, being oriented in space mainly in the binding mode I (see Supporting Information), which makes the nucleophilic attack of Ser105 unfeasible. In the case of the nonpreferential (*S*)-ester, the docking experiment revealed that the acyl moiety of the slow-reacting enantiomer is sterically accommodated in the pocket surrounded by the subsequent residues Ile189, Ala141, Leu140, and Gln157. This stems mainly from van der Waals (vdW) interactions with those surrounding hydrophobic residues as well as stabilization of the ligand−protein complexes by electrostatic interactions with the nearest neighboring polar atom of the hydrophilic residues Thr40, Gln157, and Ser105.

DOI: 10.1021/acs.joc.5b01840
J. Org. Chem. 2016, 81, 380−395

The formation of two hydrogen bonds between the unsubstituted nitrogen atom of the xanthine moiety and the hydroxy side chains of Thr40 and Ser105 residues (S1) pulled the acyl moiety of the (*S*)-ester far away from the catalytic triad and the oxyanion hole. Moreover, analysis of the second nonpreferential complex of the (*S*)-ester (S2) revealed that CAL-B could not accommodate the (*S*)-enantiomer in a catalytically active configuration as easily as the (*R*)-enantiomer owing to the very strong quaternary electrostatic interaction that occurred. In this context, the carbonyl group of the xanthine ring is stabilized through Coulombic interactions with the amide side chain of Gln157 as well as intermolecular hydrogen bonding with Thr40 and Ser105, respectively. The additional hydrogen bond between the carbonyl oxygen of the ligand acyl moiety and the carboxylic group of the Ile189 residue is believed to maintain the (*S*)-ester in its 'uncatalytical accommodation'. The above-mentioned hydrogen bonding network is considered to play an important role in (*S*)-ligand binding and, thus, might impede access to the carbonyl group of the resolved substrate (±)-**4b** in the case of the slow-reacting (*S*)-enantiomer.

In summary, the docking results unambiguously revealed that the asymmetric environment in the lipase active-site force stereoselective methanolysis of one of the (±)-**4b** enantiomers since the carbonyl group of the alkyl side chain is situated definitely much closer to the catalytic residues in the (*R*)-ester complex than in the (*S*)-ester counterpart. This conformational difference suggests a faster transformation of the (*R*)-ester over (*S*)-ester which certainly correlates to the high *E*-values obtained experimentally. Another evident discriminating factor illustrated in Figure 3 is related to the interactions between docked substrate enantiomers and the amino acid residues of the oxyanion hole. One can see that, for the slow-reacting enantiomer, all of the generated conformers are not able to place their potential oxyanion species in the oxyanion hole, with a consequent energy destabilization as compared to the fast-reacting counterpart, where stabilizing hydrogen bonds exists particularly between the oxyanions and Thr40 residue. Based on the results of the molecular docking simulation, we have proven that this method can be successfully used to predict the stereopreference of lipases used in biotransformations, and thus it could be helpful in the determination of the absolute configuration of newly resolved chiral compounds, for which stereochemistry can not be simply assigned by XRD or NMR methodology.

CONCLUSION

In summary, a lipase-catalyzed eco-friendly, facile, and scalable approach toward preparation of the single-enantiomer drug proxyphilline was developed. This procedure includes a simple kinetic resolution strategy using immobilized lipase B from *Candida antarctica* (Novozym 435). Various enzymatic systems were employed in the critical stage of the synthetic campaign. Lipase-catalyzed transesterification methodology resulted in unfortunate outcomes, whereas hydrolysis and methanolysis proved to be very efficient. The influence of enzymatic reaction parameters such as the type of lipase, solvent system, reaction time, type of the substrate's acyl group, and scale on the stereochemical outcome of kinetic resolution was investigated in detail. To demonstrate the practical viability of this process, Novozym 435 was selected as the most appropriate lipase for preparative use at 1-, 2-, and 5-g scale, respectively. We therefore have devised a straightforward and high-yielding preparation of both enantiomeric forms of proxyphylline with ee's exceeding 89% starting from cheap and renewable material (theophilline) accomplished in a short three-step synthesis. The presented methodology has shown promising potential for use in industry, as it was established with many advantages, including high enantioselectivity, up-scaling flexibility, the mild reaction conditions, good yields, and environmental friendliness as well as the possibility of simple nonchromatographic workup. Pleasingly, Novozym 435 could be taken through at least three reaction cycles without a significant loss of activity and enantioselectivity. In addition, a rational explanation of the substrate binding mode was performed by means of Auto Dock Vina software. With the docking procedure we have explained the molecular basis of enantioselective resolution of proxyphilline butanoate (±)-**4b**. It turned out that only the (*R*)-enantiomer of (±)-**4b** fit the CAL-B binding pocket in a conformation in which its acyl group is definitely in a better position to be cleaved by CAL-B than the (*S*)-ester. On the other hand, the computational analyses revealed that the initiation of the reaction for the (*S*)-enantiomer is unfavorable and consequently the *E*-values of the reaction are very high.

EXPERIMENTAL SECTION

General Experimental Methods. Reagents and solvents were purchased from various commercial sources and were used without further purification. Methylene chloride was dried by simply allowing it to stand over activated (oven-roasted in high-vacuum) 3 Å molecular sieves [20% mass/volume (m/v) loading of the desiccant] at least for 48 h before use.[48] All nonaqueous reactions were carried out under oxygen-free argon-protective conditions using flame-dried glassware. Lipase from *Candida antarctica B* [Novozym 435 was purchased from Novo Nordisk A/S (Bagsvaerd, Denmark); Chirazyme L-2, c.-f., C2, Lyo. and Chirazyme L-2, c.-f., C3, Lyo. were both purchased from Roche], lipase from *Burkholderia* (formerly *Pseudomonas*) *cepacia* [Amano PS and Amano PS-IM were purchased from Amano Pharmaceutical Co., Ltd.], lipase from *Pseudomonas fluorescens* [Amano AK was purchased from Amano Pharmaceutical Co., Ltd.], lipase from *Thermomyces lanuginosus* [Lipozyme TL IM was purchased from Novozymes (Bagsvaerd, Denmark)], lipase from *Rhizomucor miehei* [Lipozyme RM IM was purchased from Novozymes A/S (Bagsvaerds, Denmark)]; all commercial formulations of enzymes studied herein were used without any pretreatment. Analytical scale enzymatic reactions were performed in thermo-stated glass vials (V = 4 mL) placed in an anodized aluminum reaction block (48 position, 19 mm hole depth) dedicated for circular top hot plate stirring. Melting points, uncorrected, were determined with a commercial apparatus for samples contained in rotating glass capillary tubes open on one side (1.35 mm inner diameter and 80 mm length). Analytical thin-layer chromatography was carried on TLC aluminum plates covered with silica gel of 0.2 mm thickness film containing a fluorescence indicator green 254 nm (F_{254}) and using UV light as a visualizing agent. Preparative separations were carried out by column chromatography using silica gel (230−400 mesh), with a grain size of 40−63 μm. The chromatographic analyses (GC) were performed with a commercial instrument equipped with a flame ionization detector (FID) and fitted with an HP-50+ (30 m) semipolar column (50% phenyl−50% methylpolysiloxane); helium (2 mL/min) was used as the carrier gas; retention times (t_R) are given in minutes under these conditions. The enantiomeric excesses (% ee) of the resulting esters and alcohols were determined by HPLC analysis performed on a commercial chromatograph equipped with a UV detector and the corresponding commercial Chiralcel OD-H (Diacel) chiral column using mixtures of *n*-hexane/ethanol as the mobile phase in the appropriate ratios given in the Experimental Section; the HPLC analyses were executed in an isocratic manner; flow (f) is given in mL/min; racemic alcohols and esters were used as standards; the samples (2 mg) were diluted with a mobile phase composed of *n*-hexane/EtOH (1.5 mL; 3:1, v/v).

DOI: 10.1021/acs.joc.5b01840
J. Org. Chem. 2016, 81, 380−395

Optical rotations ([α]) were measured with a commercial polarimeter in a 2 dm long cuvette at 27.5 °C using the sodium D line (λ = 589 nm); the units of the specific rotation [α] are given in (deg × mL)/(g × dm) and calculated from the following equation: [α] = (100 × α)/(l × c), where the concentration c is in g/100 mL, α is the measured value, and the path length l is in decimeters; samples were prepared in $CHCl_3$. UV spectra were measured with spectrometer for the samples prepared in absolute EtOH. ^1H and ^{13}C NMR spectra were measured with a commercial spectrometer operating at 400 MHz for ^1H and 100 MHz for ^{13}C nuclei; chemical shifts (δ) are given in parts per million (ppm) related to deuterated chloroform ($CDCl_3$, δ = 7.26) as the internal standard; signal multiplicity assignment: s, singlet; d, doublet; t, triplet; q, quartet; m, multiplet; coupling constants (J) are given in hertz (Hz); all of the ^1H and ^{13}C NMR spectra were created by a noncommercial (freeware) ACD/NMR Processor Academic Edition 12.0. High-resolution mass (HRMS) and Fourier transform mass spectrometry (FTMS) were carried out with electrospray ionization (ESI) using a Q-TOF mass spectrometer. Infrared spectra of neat samples were recorded on an FT-IR spectrophotometer equipped with an attenuated total reflectance (ATR) accessory with a monolithic diamond crystal stage and a pressure clamp; FTIR spectra were recorded in transmittance mode in the 300−4000 cm^{-1} range, in ambient air at room temperature, with 2 cm^{-1} resolution and accumulation of 32 scans.

Chemical Synthesis. *Synthesis of 7-(2-Hydroxypropyl)-1,3-dimethyl-3,7-dihydro-1H-purine-2,6-dione (±)-**3**.* The mixture composed of anhydrous theophylline **1** (10 g, 55.51 mmol), propylene oxide **2** (10 g, 0.17 mol, 12 mL), and a catalytic amount of Et_3N (954 mg, 9.44 mmol, 1.3 mL) in MeOH (50 mL) was stirred for 4 h under reflux conditions until the suspension become fully dissolved. Next, half of the volatiles were evaporated and the flask was stored in the fridge for 2 h until the content solidified. Subsequently, the resulting solid was filtered off and washed with cold MeOH (50 mL) yielding desired product (±)-**3** as a white crystalline solid (9.77 g, 41 mmol, 74%).

White solid; yield 74%; mp 136−137 °C (MeOH) [lit.[41] 135−136 °C ($EtOH_{anh.}$)]; R_f [$CHCl_3$/MeOH (90:10, v/v), silica gel plate] 0.42 or R_f [$CHCl_3$/MeOH (95:5, v/v), silica gel plate] 0.24; ^1H NMR ($CDCl_3$, 400 MHz) δ: 1.24 (d, J = 6.3 Hz, 3H), 3.15 (br. s., 1H), 3.33 (s, 3H), 3.50 (s, 3H), 4.05 (dd, J = 14.0, 7.7 Hz, 1H), 4.13−4.23 (m, 1H), 4.44 (dd, J = 13.8, 2.9 Hz, 1H), 7.60 (s, 1H); ^{13}C NMR ($CDCl_3$, 100 MHz) δ: 20.5, 28.0, 29.8, 53.7, 66.4, 107.0, 142.2, 148.6, 151.3, 155.6; FTMS (ESI-TOF) m/z: [M + H]$^+$ Calcd for $C_{10}H_{15}N_4O_3^+$ 239.11442, Found 239.11361; HRMS (ESI-TOF) m/z: [M + H]$^+$ Calcd for $C_{10}H_{15}N_4O_3^+$ 239.1144, Found 239.1130; HRMS (ESI-TOF) m/z: [M + Na]$^+$ Calcd for $C_{10}H_{14}N_4O_3Na^+$ 261.0964, Found 261.0955. Anal. calcd for $C_{10}H_{14}N_4O_3$: C, 50.41; H, 5.92; N, 23.52. Found: C, 50.42; H, 5.98; N, 23.59. FTIR ν_{max}(neat): 3486.9, 1697.1, 1656.8, 1547.7, 1472.1, 1457.8, 1425.3, 1400.5, 1373.4, 1359.2, 1321.0, 1287.7, 1249.9, 1223.2, 1194.1, 1140.5, 1086.7, 1071.5, 1023.4, 971.2, 940.6, 887.4, 846.7, 759.3, 746.7, 669.0, 619.1, 536.5, 509.3, 476.7, 443.7, 422.3; UV/vis: λ_{max} = 273 nm (EtOH); GC [230−260 (10 °C/min)]: t_R = 4.80 min or [200−260 (10 °C/min)]: t_R = 6.83 min or [170−260 (3 °C/min)]: t_R = 19.88 min; HPLC [n-hexane/EtOH (90:10, v/v); f = 0.5 mL/min]: t_R = 40.390 (S) and 44.107 (R).

*Synthesis of Racemic 1-(1,3-Dimethyl-2,6-dioxo-1,2,3,6-tetrahydro-7H-purin-7-yl)propan-2-yl Acetate (±)-**4a**.* To the solution of 7-(2-hydroxypropyl)-1,3-dimethyl-3,7-dihydro-1H-purine-2,6-dione (proxyphylline) (±)-**3** (2 g; 8.39 mmol) in dry CH_2Cl_2 (20 mL), DMAP (205 mg; 1.68 mmol) was added. Next, acetic anhydride (4.28 g, 54.57 mmol, 3.97 mL) was dissolved in dry CH_2Cl_2 (10 mL) and added dropwise to the reaction mixture. Afterward, the resulting mixture was stirred at room temperature for 30 min and then quenched with water (35 mL). The water phase was extracted with CH_2Cl_2 (3 × 30 mL), and the combined organic layers were washed with saturated $NaHCO_3$ solution (10 × 100 mL) and dried over Na_2SO_4. The solvent was removed under reduced pressure, and the crude product was purified by column chromatography on silica gel using $CHCl_3$/MeOH (95:5, v/v) as the eluent, evaporated to dryness, and subsequently washed with cold MeOH (10 mL) yielding product (±)-**4a** as a white crystalline solid (2.23 g, 7.96 mmol, 95%).

White solid; yield 95%; mp 51−52.5 °C (crop I, MeOH), mp 84.5−86 °C (crop II, MeOH), mp 92−93.5 °C (crop III, MeOH); R_f [$CHCl_3$/MeOH (95:5, v/v), silica gel plate] 0.67; ^1H NMR ($CDCl_3$, 400 MHz) δ: 1.29 (d, J = 6.3 Hz, 3H), 1.97 (s, 3H), 3.38 (s, 3H), 3.57 (s, 3H), 4.23 (dd, J = 14.2, 8.1 Hz, 1H), 4.59 (dd, J = 14.2, 2.9 Hz, 1H), 5.20−5.29 (m, 1H), 7.54 (s, 1H); ^{13}C NMR ($CDCl_3$, 100 MHz) δ: 17.2, 21.0, 27.9, 29.8, 50.7, 69.1, 106.9, 141.4, 148.5, 151.5, 155.1, 169.8; FTMS (ESI-TOF) m/z: [M + H]$^+$ Calcd for $C_{12}H_{17}N_4O_4^+$ 281.12498, Found 281.12420; HRMS (ESI-TOF) m/z: [M + H]$^+$ Calcd for $C_{12}H_{17}N_4O_4^+$ 281.1250, Found 281.1257; HRMS (ESI-TOF) m/z: [M + Na]$^+$ Calcd for $C_{12}H_{16}N_4O_4Na^+$ 303.1069, Found 303.1060; Anal. Calcd for $C_{12}H_{16}N_4O_4$: C, 51.42; H, 5.75; N, 19.99. Found: C, 51.60; H, 5.75; N, 20.02; FTIR ν_{max}(neat): 3122.4, 3021.6, 1737.0, 1705.6, 1658.4, 1550.6, 1472.8, 1455.6, 1405.8, 1367.2, 1290.0, 1224.2, 1190.0, 1134.3, 1069.2, 1026.8, 974.2, 961.1, 932.6, 924.5, 894.2, 852.6, 821.8, 759.6, 742.9, 664.3, 640.4, 615.2, 607.8, 509.1, 457.8, 425.6; UV/vis: λ_{max} = 273 nm (EtOH); GC [230−260 (10 °C/min)]: t_R = 4.86 min or [170−260 (3 °C/min)]: t_R = 20.46 min; HPLC [n-hexane/EtOH (90:10, v/v); f = 0.8 mL/min]: t_R = 21.429 (S) and 22.908 (R) or 21.080 (S) and 23.755 (R); HPLC [n-hexane/EtOH (95:5, v/v); f = 0.8 mL/min]: t_R = 38.804 (S) and 48.448 (R).

*Synthesis of Racemic 1-(1,3-Dimethyl-2,6-dioxo-1,2,3,6-tetrahydro-7H-purin-7-yl)propan-2-yl Butanoate (±)-**4b**. Method A.* To the solution of 7-(2-hydroxypropyl)-1,3-dimethyl-3,7-dihydro-1H-purine-2,6-dione (proxyphylline) (±)-**3** (1.5 g; 6.30 mmol) in dry CH_2Cl_2 (20 mL), Et_3N (955 mg; 9.44 mmol, 1.15 mL) and DMAP (10 mg; 0.13 mmol) were added. The mixture was cooled to 0−5 °C in an ice bath. Next, butanoyl chloride (1 g, 9.44 mmol) dissolved in dry CH_2Cl_2 (10 mL) was added dropwise to the reaction mixture. Afterward, the cooling bath was removed, and the resulting mixture was stirred at room temperature overnight and then quenched with water (35 mL). The water phase was extracted with CH_2Cl_2 (3 × 30 mL), and the combined organic layers were washed with a saturated solution of $NaHCO_3$ (2 × 50 mL) and dried over Na_2SO_4. After the drying agent was filtered off, the solvent was evaporated under reduced pressure, and the crude product was purified by column chromatography on silica gel using $CHCl_3$/MeOH (95:5, v/v) as the eluent, thus yielding the product (±)-**4b** as a yellowish oil (1.63 g, 5.29 mmol, 84%).

Method B. To the solution of 7-(2-hydroxypropyl)-1,3-dimethyl-3,7-dihydro-1H-purine-2,6-dione (proxyphylline) (±)-**3** (200 mg; 0.84 mmol) in MTBE (3 mL), Novozym 435 [40 mg, 5% w/w (catalyst/substrate (±)-**3**)] and vinyl butanoate (363 mg; 3.78 mmol) were added in one portion and vigorously stirred (1000 rpm) at room temperature overnight. Next, the enzyme was filtered off and washed with MTBE (15 mL); the permeate was partially condensed under reduced pressure, and the thus obtained crude product was purified by column chromatography on silica gel using $CHCl_3$/MeOH (95:5, v/v) as eluent yielding desired ester (±)-**4b** as a yellowish oil (252 mg; 0.82 mmol; 97%).

Yellowish oil; yield 94% (corrected on the basis of the NMR assignment); R_f [$CHCl_3$/MeOH (95:5, v/v), silica gel plate] 0.76; ^1H NMR ($CDCl_3$, 400 MHz) δ: 0.84 (t, J = 7.5 Hz, 3H), 1.28 (d, J = 6.3 Hz, 3H), 1.48−1.59 (m, 2H), 2.18 (td, J = 7.5, 2.9 Hz, 2H), 3.37 (s, 3H), 3.55 (s, 3H), 4.24 (dd, J = 14.3, 8.2 Hz, 1H), 4.57 (dd, J = 14.1, 2.8 Hz, 1H), 5.20−5.30 (m, 1H), 7.52 (s, 1H); ^{13}C NMR ($CDCl_3$, 100 MHz) δ: 13.5, 17.2, 18.2, 27.9, 29.8, 36.1, 50.7, 68.8, 106.9, 141.4, 148.5, 151.5, 155.1, 172.4; FTMS (ESI-TOF) m/z: [M + H]$^+$ Calcd for $C_{14}H_{21}N_4O_4^+$ 309.15628, Found 309.15556; HRMS (ESI-TOF) m/z: [M + H]$^+$ Calcd for $C_{14}H_{21}N_4O_4^+$ 309.1563, Found 309.1553; HRMS (ESI-TOF) m/z: [M + Na]$^+$ Calcd for $C_{14}H_{20}N_4O_4Na^+$ 331.1382, Found 331.1373; FTIR ν_{max}(neat): 2964.9, 1735.2, 1701.1, 1650.6, 1604.0, 1546.3, 1473.5, 1456.1, 1426.9, 1407.5, 1374.9, 1288.3, 1252.1, 1228.3, 1172.8, 1133.5, 1087.0, 1066.7, 1024.9, 975.7, 761.1, 747.0, 620.7, 510.5, 474.1, 423.3; UV/vis: λ_{max} = 274 nm (EtOH); GC [200−260 (10 °C/min)]: t_R = 8.48 min; HPLC [n-hexane/EtOH (97:3, v/v); f = 0.4 mL/min]: t_R = 77.640 (S) and 81.404 (R) or 83.323 (S) and 87.116 (R).

DOI: 10.1021/acs.joc.5b01840
J. Org. Chem. 2016, 81, 380−395

*Synthesis of Racemic 1-(1,3-Dimethyl-2,6-dioxo-1,2,3,6-tetrahydro-7H-purin-7-yl)propan-2-yl Decanoate (±)-**4c**.* To the solution of 7-(2-hydroxypropyl)-1,3-dimethyl-3,7-dihydro-1*H*-purine-2,6-dione (proxyphylline) (±)-**3** (200 mg; 0.84 mmol) in dry CH_2Cl_2 (2 mL), Et_3N (127 mg; 1.26 mmol, 0.13 mL) and DMAP (10 mg; 0.08 mmol) were added in a gentle flow of argon. Next, the mixture was cooled to 0−5 °C in an ice bath, and decanoyl chloride (240 mg; 1.26 mmol) dissolved in dry CH_2Cl_2 (1 mL) was added dropwise to the reaction mixture by using a syringe. Afterward, the cooling bath was removed, and the resulting mixture was stirred at room temperature overnight and then quenched with water (5 mL). The water phase was extracted with CH_2Cl_2 (3 × 5 mL), and the combined organic layers were washed with a saturated solution of $NaHCO_3$ (10 mL) and brine (10 mL) and dried over Na_2SO_4. The solvent was evaporated under reduced pressure, and the crude product was purified by preparative-layer chromatography (PLC) using SiO_2-covered plates and a mixture of *n*-hexane/acetone (1.5:1.0, v/v) as the eluent, thus obtaining desired ester (±)-**4c** as a colorless oil (273 mg; 0.69 mmol; 83%).

Colorless oil; yield 83%; R_f [*n*-hexane/acetone (1.5:1, v/v), silica gel plate] 0.58; ^{1}H NMR ($CDCl_3$, 400 MHz) δ: 0.85 (t, J = 6.9 Hz, 3H), 1.16−1.26 (m, 10H), 1.28 (d, J = 6.3 Hz, 3H), 1.44−1.57 (m, 2H), 2.13−2.17 (m, 2H), 2.20 (td, J = 7.6, 3.6 Hz, 2H), 3.38 (s, 3H), 3.56 (s, 3H), 4.24 (dd, J = 14.2, 8.1 Hz, 1H), 4.57 (dd, J = 14.2, 2.9 Hz, 1H), 5.18−5.32 (m, 1H), 7.51 (s, 1H); ^{13}C NMR ($CDCl_3$, 100 MHz) δ: 14.0, 17.6, 22.5, 24.7, 27.9, 28.9, 29.1, 29.1, 29.3, 29.7, 31.7, 34.2, 50.7, 68.8, 106.8, 141.4, 148.5, 151.4, 155.1, 172.6; FTMS (ESI-TOF) m/z: $[M + H]^+$ Calcd for $C_{20}H_{33}N_4O_4^+$ 393.25018, Found 393.24940; HRMS (ESI-TOF) m/z: $[M + H]^+$ Calcd for $C_{20}H_{33}N_4O_4^+$ 393.2502, Found 393.2490; HRMS (ESI-TOF) m/z: $[M + Na]^+$ Calcd for $C_{20}H_{32}N_4O_4Na^+$ 415.2321, Found 415.2315; FTIR ν_{max}(neat): 2926.05, 2854.9, 1735.6, 1701.7, 1654.6, 1604.3, 1547.9, 1473.1, 1457.3, 1427.2, 1408.2, 1375.5, 1288.9, 1228.7, 1164.3, 1134.3, 1068.8, 1025.2, 976.5, 761.7, 748.7, 620.6, 509.7, 473.7, 443.6, 423.9; UV/vis: λ_{max} = 273 nm (EtOH); GC analysis failed, as (±)-**4c** is nonvolatile in the recommended temperature range limits (<260 °C) recommended for the available column; HPLC analysis also failed, as (±)-**4c** is not resolvable on a Chiralcel OD-H column.

General Procedure for Analytical-Scale KR of (±)-3 Using Lipase-Catalyzed Transesterification−Enzyme Screening. To the solution of racemic alcohol (±)-**3** (100 mg, 0.42 mmol) in $CHCl_3$ (1 mL), the respective commercial lipase formulation [20 mg, 20% w/w (catalyst/substrate)] and vinyl acetate (415 mg, 4.83 mmol, 0.5 mL) were added in one portion. The reaction mixture was stirred (500 rpm) in a thermo-stated screw-capped test glass vial (V = 4 mL) at 25 °C. The progress of the KR was monitored by GC analysis, and after reaching appropriate conversion the reaction was terminated by filtering off the enzyme. After washing the enzyme with $CHCl_3$ (10 mL), collected chloroform solutions were concentrated under reduced pressure, and the residue was purified by column chromatography on silica gel using a mixture of $CHCl_3$/MeOH (95:5, v/v) as the eluent, thus affording the respective resolution products [alcohol (*S*)-(+)-**3** and the acetate (*R*)-(−)-**4a**]. Next, to obtain necessary information concerning values of % conversion, enantiomeric excess (% ee), and enantioselectivity (E), the HPLC analyses were performed. For optically active alcohol (*S*)-(+)-**3** an extra derivatization procedure was required (see section *Analysis of enantiomeric purity of (S)-(+)-3 or (R)-(−)-3*). For additional data, see Table 1.

General Procedure for Analytical-Scale KR of (±)-4a Using Lipase-Catalyzed Alcoholysis−Selection of Lipase and Reaction Medium. Methanol (114 mg, 3.57 mmol, 0.15 mL) and the appropriate lipase [20 mg, 20% w/w (catalyst/substrate)] were added to the solution of racemic acetate (±)-**4a** (100 mg, 0.36 mmol) in the respective organic solvent (1 mL) and stirred (500 rpm) in a thermo-stated screw-capped test glass vial (V = 4 mL) at 25 °C for the time necessary to achieve good kinetic resolution (see Table 2 and Table 3). Further manipulations were carried out by analogy with the previously described procedure for the enzyme screening (see section *enzyme screening*).

General Procedure for Analytical-Scale Enzymatic KR of (±)-4b − Alcoholysis vs Hydrolysis. Methanol (104 mg, 3.24 mmol, 0.13 mL) or water (58 mg, 3.24 mmol, 0.58 mL) or 1 M Tris-HCl buffer (58 mg, 3.24 mmol, 0.58 mL, pH 7.5) and Novozym 435 [20 mg, 20% w/w (catalyst/substrate)] were added to the solution of racemic butanoate (±)-**4b** (100 mg, 0.36 mmol) in CH_3CN (1 mL). The reaction mixture was stirred (500 rpm) in a thermo-stated screw-capped test glass vial (V = 4 mL) at 25 °C for the necessary time to achieve good kinetic resolution (see Tables 4 and 5). For hydrolytic attempts, after enzyme removal and washing the filter cake with $CHCl_3$ (10 mL), the permeate was additionally dried over Na_2SO_4, filtered off, and evaporated to dryness under reduced pressure. The residue was separated by column chromatography on silica gel using $CHCl_3$/MeOH (95:5, v/v) as the eluent yielding optically active products [ester (*S*)-(+)-**4b** and alcohol (*R*)-(−)-**3**].

General Procedure for 2-g Scale (Novozym 435)-Catalyzed KR of (±)-4b by Methanolysis. The reaction mixture containing racemic ester (±)-**4b** (2 g, 6.49 mmol), CH_3CN (20 mL), MeOH (2.08 g, 64.87 mmol, 2.63 mL), and Novozym 435 [400 mg, 20% w/w (catalyst/substrate (±)-**3**)] was stirred (500 rpm, IKA RCT basic) in a round-bottomed flask (50 mL) at 25 °C for the appropriate time (see Table 6). The reaction was followed by GC analysis until ca. 50% substrate conversion was reached. The enzyme was then removed by filtration and washed with $CHCl_3$ (50 mL). Next, the combined solutions were evaporated under reduced pressure, and the crude products were purified by column chromatography on silica gel using a gradient of $CHCl_3$/MeOH (95:5, 90:10, v/v) mixture as the eluent, affording the corresponding optically active butanoate (*S*)-(+)-**4b** (93−94% yield, 88−100% ee) and alcohol (*R*)-(−)-**3** (89−93% yield, 95−97% ee). The given isolated yields are based on the maximum amount which can be stoichiometrically obtained, that is, based on half the amount of (±)-**4b** used in the case of the reaction stopped at 50% conversion. The results of enzymatic KR for the 1- and 2-g scale, including products optical rotation values, are collected in Table 6.

General Procedure for 5-g Scale (Novozym 435)-Catalyzed KR of (±)-4b by Methanolysis. The reaction mixture containing racemic ester (±)-**4b** (5 g, 16.22 mmol), CH_3CN (50 mL), MeOH (5.20 g, 0.16 mol, 6.60 mL), and Novozym 435 [1 g, 20% w/w (catalyst/substrate (±)-**3**)] was stirred (500 rpm) in a round-bottomed flask (250 mL) equipped with a Teflon-coated magnetic stirring bar (20 × 5 mm, 2 g) at 25 °C for the appropriate time (see Table 6). The course of the reaction was followed by GC analysis until ca. 50% conversion was reached. Enzymatic KR was stopped by filtering off the enzyme together with the precipitated alcohol product (*R*)-(−)-**3**. The permeate containing dissolved unreacted butanoate (*S*)-(+)-**4b** and residues of the formed alcohol (*R*)-(−)-**3** was partially concentrated in vacuo and left in a refrigerator for 3 h, and afterward, the resulting white precipitate of the alcohol was collected by filtration. The filtrate was again concentrated and passed through a short silica pad eluting with a mixture of $CHCl_3$/MeOH (80:20, v/v) to obtain optically active butanoate (*S*)-(+)-**4b** (90−93% yield, from 97% ee to >99% ee). The alcohol (*R*)-(−)-**3** was also recovered from the filter cake (enzyme + precipitate) by washing it with $CHCl_3$ (50 mL), evaporating the solvent to dryness, adding a portion of MeOH, and, finally, leaving the content in the fridge until a white precipitate of the alcohol was formed. Both obtained crops were collected and purified by recrystallization from MeOH to give enantiomerically enriched alcohols (*R*)-(−)-**3** (91−94% yield, 89−96% ee). The experimental conditions and the results of enzymatic KR reactions for the 5-g scale, including the product optical rotation values, are collected in Table 6. Physical, spectroscopic, and analytical data are identical with the corresponding racemic standard compounds.

Determination of Enantiomeric Purity of (*S*)-(+)-3 or (*R*)-(−)-3. The enantiomeric excess (% ee) of the alcohol enantiomers (*S*)-(+)-**3** or (*R*)-(−)-**3** (20 mg, 0.08 mmol) was determined by HPLC on a chiral phase after derivatization to the corresponding acetate (*S*)-(+)-**4a** or (*R*)-(−)-**4a**, which was performed by addition of a catalytic amount of DMAP (3 mg) and a 5-fold excess of acetic anhydride (43 mg, 0.42 mmol, 40 μL) dissolved in CH_2Cl_2 (0.4 mL) and vigorous stirring for 15 min at ambient temperature. Next, a portion of CH_2Cl_2 (0.8 mL) was added followed by washing with saturated $NaHCO_3$ (4 × 1 mL) until effervescence ceased. Subsequently, the organic phase

DOI: 10.1021/acs.joc.5b01840
J. Org. Chem. 2016, 81, 380−395

was separated and dried over a mixture of anhydrous K_2CO_3, Na_2SO_4, and $MgSO_4$, and after filtration of the drying agents the solvent residual was removed under vacuum. The respective crude acetate was subsequently dissolved in a mixture of *n*-hexane/EtOH (1.5 mL, 3:1, v/v) and directly injected without further cleanup. An alternative method of the sample purification was based on short column chromatography on silica gel in the eluent system containing a mixture of $CHCl_3$/MeOH (90:10, v/v).

Docking Studies. Computer molecular dynamics simulations (docking studies) to determine favorable ligand binding geometries for the substrates were carried out using AutoDock Vina vs the 1.1.2 program for Windows (http://autodock.scripps.edu/).[45] Ligand molecules were prepared with ChemAxon MarvinSketch vs 14.9.1.0 (http://www.chemaxon.com/marvin/) and saved as .PDB or .mol2 files, respectively. Gasteiger partial charges were calculated with AutoDock Tools vs 1.5.6 (ADT, S3 http://mgltools.scripps.edu/),[49] and the final ligand files were prepared in PDBQT format. The crystallographic structures of lipase from *Candida antarctica B* (PDB code 1TCA)[47] were downloaded from Brookhaven RCSB Protein Data Bank (PDB, http://www.rcsb.org/pdb/). The crude protein .pdb file was prepared by UCSF Chimera vs 1.9 package (http://www.cgl.ucsf.edu/chimera/).[50] All nonstandard (nonprotein) molecules including the two sugar units (NAG) and 286 crystal waters were removed, the polar hydrogen atoms were added, and Gasteiger charges were calculated with the AutoDock Tools 1.5.6 package.[45] With use of AutoGrid, a searching grid box was set in the appropriate size before docking. The box center was set at catalytic Ser105 of CAL-B. Docking was performed in a 40 × 40 × 40 unit grid box centered on the enzyme active site (center_x = −3.144; center_y = 21.093; center_z = 12.736) with a grid spacing of 0.325 Å. Each docking was performed with an exhaustiveness level of 48. For each ligand molecule 100 independent runs were performed, using the Lamarckian genetic algorithm (GA), with at most 106 energy evaluations and a maximum number of generations of >27 000 $Å^3$ (the search space volume). The remaining GA parameters were set as default. The docking configurations of each ligand were ranked on the basis of free binding energy (kcal/mol). The best nine poses (modes) were selected according to AutoDock Vina scoring functions mainly based on binding energies and show mutual affinity (kcal/mol). Each selected binding mode was manually inspected in order to select only productive conformations where the substrate assumes a Near Attack Conformation (NAC) compatible with the attack of the catalytic serine (Ser105) to the carbon atom of the acyl group of the ligand. The molecular modeling treated the two isomers (*R* and *S*) independently, and the docking procedure used both isomers for each compound. The docked ligand conformations and the subsequent analysis of intermolecular interactions in the CAL-B active site were performed with The PyMOL Molecular Graphics System software, version 1.3, Schrödinger, LLC (https://www.pymol.org/). For docking scoring see the Supporting Information.

■ ASSOCIATED CONTENT

Supporting Information

The Supporting Information is available free of charge on the ACS Publications website at DOI: 10.1021/acs.joc.5b01840.

Copies of ^1H NMR, ^{13}C NMR, HRMS, FTMS, IR, UV/vis spectra and HPLC, GC chromatograms of all compounds as well as docking scoring (PDF)

■ AUTHOR INFORMATION

Corresponding Author

*E-mail: pawel_borowiecki@onet.eu; pborowiecki@ch.pw.edu.pl.

Notes

The authors declare no competing financial interest.

■ ACKNOWLEDGMENTS

Author wish to acknowledge National Science Center of Poland (No. 2014/13/N/ST5/01589) for the financial support. This work was partially supported by the Warsaw University of Technology, Faculty of Chemistry.

■ REFERENCES

(1) (a) Agranat, I.; Caner, H.; Caldwell, J. *Nat. Rev. Drug Discovery* **2002**, *1*, 753−768. (b) Caldwell, J. *Hum. Psychopharmacol.* **2001**, *16*, S67−S71.

(2) (a) Kasprzyk-Hordern, B. *Chem. Soc. Rev.* **2010**, *39*, 4466−4503. (b) Mentel, M.; Blankenfeldt, W.; Breinbauer, R. *Angew. Chem., Int. Ed.* **2009**, *48*, 9084−9087. (c) Carey, J. S.; Laffan, D.; Thomson, C.; Williams, M. T. *Org. Biomol. Chem.* **2006**, *4*, 2337−2347.

(3) Branch, S.; Subramanian, G. In *International Regulation of Chiral Drugs. Chiral Separation Techniques. A Practical Approach*; Subramanian, G., Branch, S., Eds.; Wiley-VCH: Weinheim, 2001; pp 319−342.

(4) (a) Lorenz, H.; Seidel-Morgenstern, A. *Angew. Chem., Int. Ed.* **2014**, *53*, 1218−12150. (b) Tzschucke, C. C.; Markert, C.; Bannwarth, W.; Roller, S.; Hebel, A.; Haag, R. *Angew. Chem., Int. Ed.* **2002**, *41*, 3964−4000.

(5) Holmquist, M. *Curr. Protein Pept. Sci.* **2000**, *1*, 209−235.

(6) (a) Gupta, R.; Kumari, A.; Syal, P.; Singh, Y. *Prog. Lipid Res.* **2015**, *57*, 40−54. (b) Stergiou, P. Y.; Foukis, A.; Filippou, M.; Koukouritaki, M.; Parapouli, M.; Theodorou, L. G.; Hatziloukas, E.; Afendra, A.; Pandey, A.; Papamichael, E. M. *Biotechnol. Adv.* **2013**, *31*, 1846−1859. (c) Ghanem, A. *Tetrahedron* **2007**, *63*, 1721−1754.

(7) (a) Salihu, A.; Alam, M. Z. *Process Biochem.* **2015**, *50*, 86−96. (b) Adlercreutz, P. *Chem. Soc. Rev.* **2013**, *42*, 6406−6436. (c) Zaks, A.; Klibanov, A. M. *Proc. Natl. Acad. Sci. U. S. A.* **1985**, *82*, 3192−3196. (d) Sym, E. A. *Biochem. J.* **1936**, *30*, 609−617.

(8) (a) Rodrigues, J. V.; Ruivo, D.; Rodríguez, A.; Deive, F. J.; Esperança, J. M. S. S.; Marrucho, I. M.; Gomes, C. M.; Rebelo, L. P. N. *Green Chem.* **2014**, *16*, 4520−4523. (b) De Diego, T.; Manjón, A.; Lozano, P.; Vaultier, M.; Iborra, J. L. *Green Chem.* **2011**, *13*, 444−451. (c) Filice, M.; Guisan, J. M.; Palomo, J. M. *Green Chem.* **2010**, *12*, 1365−1369.

(9) (a) Corici, L.; Pellis, A.; Ferrario, V.; Ebert, C.; Cantone, S.; Gardossi, L. *Adv. Synth. Catal.* **2015**, *357*, 1763−1774. (b) El-Boulifi, N.; Ashari, S. E.; Serrano, M.; Aracil, J.; Martinez, M. *Enzyme Microb. Technol.* **2014**, *55*, 128−132. (c) Pyo, S.-H.; Persson, P.; Lundmark, S.; Hatti-Kaul, R. *Green Chem.* **2011**, *13*, 976−982.

(10) (a) Guan, Z.; Li, L.-Y.; He, Y.-H. *RSC Adv.* **2015**, *5*, 16801−16814. (b) Zhang, Y.; Vongvilai, P.; Sakulsombat, M.; Fischer, A.; Ramström, O. *Adv. Synth. Catal.* **2014**, *356*, 987−992. (c) Kapoor, M.; Gupta, M. N. *Process Biochem.* **2012**, *47*, 555−569.

(11) (a) Wu, Q.; Soni, P.; Reetz, M. T. *J. Am. Chem. Soc.* **2013**, *135*, 1872−1881. (b) Reetz, M. T. *J. Am. Chem. Soc.* **2013**, *135*, 12480−12496. (c) Ema, T.; Nakano, Y.; Yoshida, D.; Kamata, S.; Sakai, T. *Org. Biomol. Chem.* **2012**, *10*, 6299−6308. (d) Brundiek, H. B.; Evitt, A. S.; Kourist, R.; Bornscheuer, U. T. *Angew. Chem., Int. Ed.* **2012**, *51*, 412−414.

(12) (a) Barbosa, O.; Ortiz, C.; Berenguer-Murcia, A.; Torres, R.; Rodrigues, R. C.; Fernandez-Lafuente, R. *Biotechnol. Adv.* **2015**, *33*, 435−456. (b) Souza, R. L.; Lima, R. A.; Coutinho, J. A. P.; Soares, C. M. F.; Lima, Á. S. *Sep. Purif. Technol.* **2015**, *155*, 118. (c) Souza, R. L.; Lima, R. A.; Coutinho, J. A. P.; Soares, C. M. F.; Lima, Á. S. *Process Biochem.* **2015**, *50*, 1459−1467.

(13) (a) Zhao, D.; Peng, C.; Zhou, J. *Phys. Chem. Chem. Phys.* **2015**, *17*, 840−850. (b) Nascimento, M. d. G.; da Silva, J. M. R.; da Silva, J. C.; Alves, M. M. *J. Mol. Catal. B: Enzym.* **2015**, *112*, 1−8. (c) Esmaeilnejad-Ahranjani, P.; Kazemeini, M.; Singh, G.; Arpanaei, A. *RSC Adv.* **2015**, *5*, 33313−33327. (d) Adlercreutz, P. *Chem. Soc. Rev.* **2013**, *42*, 6406−6436.

(14) (a) Su, E.; Wei, D. *J. Agric. Food Chem.* **2014**, *62*, 6375−6381. (b) Qin, X. L.; Yang, B.; Huang, H. H.; Wang, Y. H. *J. Agric. Food*

DOI: 10.1021/acs.joc.5b01840
J. Org. Chem. 2016, 81, 380−395

Chem. **2012**, *60*, 2377−2384. (c) Teichert, S. A.; Akoh, C. C. *J. Agric. Food Chem.* **2011**, *59*, 9588−9595.
(15) (a) Hertzberg, R.; Monreal Santiago, G.; Moberg, C. *J. Org. Chem.* **2015**, *80*, 2937−2941. (b) Dwivedee, B. P.; Ghosh, S.; Bhaumik, J.; Banoth, L.; Chand Banerjee, U. *RSC Adv.* **2015**, *5*, 15850−15860. (c) Ramesh, P.; Harini, T.; Fadnavis, N. W. *Org. Process Res. Dev.* **2015**, *19*, 296−301. (d) Fonseca, T. d. S.; Silva, M. R. d.; de Oliveira, M. d. C. F.; Lemos, T. L. G. d.; Marques, R. d. A.; de Mattos, M. C. *Appl. Catal., A* **2015**, *492*, 76−82. (e) Sayin, S.; Akoz, E.; Yilmaz, M. *Org. Biomol. Chem.* **2014**, *12*, 6634−6642. (f) Borowiecki, P.; Paprocki, D.; Dranka, M. *Beilstein J. Org. Chem.* **2014**, *10*, 3038−3055.
(16) (a) Krumlinde, P.; Bogár, K.; Bäckvall, J. E. *J. Org. Chem.* **2009**, *74*, 7407−7410. (b) Zhou, R.; Xu, J.-H. *Biochem. Eng. J.* **2005**, *23*, 11−15. (c) Cheng, Y.-C.; Tsai, S.-W. *Tetrahedron: Asymmetry* **2004**, *15*, 2917−2920.
(17) (a) Lu, P.; Herrmann, A. T.; Zakarian, A. *J. Org. Chem.* **2015**, *80*, 7581−7589. (b) Beretta, R.; Giambelli Gallotti, M.; Penne, U.; Porta, A.; Gil Romero, J. F.; Zanoni, G.; Vidari, G. *J. Org. Chem.* **2015**, *80*, 1601−1609. (c) Risi, R. M.; Maza, A. M.; Burke, S. D. *J. Org. Chem.* **2015**, *80*, 204−216. (d) Yamamoto, H.; Takagi, Y.; Oshiro, T.; Mitsuyama, T.; Sasaki, I.; Yamasaki, N.; Yamada, A.; Kenmoku, H.; Matsuo, Y.; Kasai, Y.; Imagawa, H. *J. Org. Chem.* **2014**, *79*, 8850−8855.
(18) (a) Wei, C.; Fu, X.-F.; Wang, Z.; Yu, X.-J.; Zhang, Y.-J.; Zheng, J.-Y. *J. Mol. Catal. B: Enzym.* **2014**, *106*, 90−94. (b) Torres, P.; Kunamneni, A.; Ballesteros, A.; Plou, F. J. *Open Food Sci. J.* **2008**, *2*, 1−9. (c) Torres, P.; Reyes-Duarte, D.; López-Cortés, N.; Ferrer, M.; Ballesteros, A.; Plou, F. J. *Process Biochem.* **2008**, *43*, 145−153.
(19) Ansorge-Schumacher, M. B.; Thum, O. *Chem. Soc. Rev.* **2013**, *42*, 6475−6490.
(20) (a) Martins, A. B.; da Silva, A. M.; Schein, M. F.; Garcia-Galan, C.; Záchia Ayub, M. A.; Fernandez-Lafuente, R.; Rodrigues, R. C. *J. Mol. Catal. B: Enzym.* **2014**, *105*, 18−25. (b) Lozano, P.; Bernal, J. M.; Navarro, A. *Green Chem.* **2012**, *14*, 3026−3033. (c) Brenna, E.; Fuganti, C.; Gatti, F. G.; Serra, S. *Chem. Rev.* **2011**, *111*, 4036−4072.
(21) (a) Cao, M.; Fonseca, L. M.; Schoenfuss, T. C.; Rankin, S. A. *J. Agric. Food Chem.* **2014**, *62*, 5726−5733. (b) Okino-Delgado, C. H.; Fleuri, L. F. *Food Chem.* **2014**, *163*, 103−107. (c) Ferreira-Dias, S.; Sandoval, G.; Plou, F.; Valero, F. *Electron. J. Biotechnol.* **2013**, *16*, 3−5.
(22) (a) Wang, J.; Wang, S.; Li, Z.; Gu, S.; Wu, X.; Wu, F. *J. Mol. Catal. B: Enzym.* **2015**, *111*, 21−28. (b) Zheng, M.-M.; Wang, L.; Huang, F.-H.; Guo, P.-M.; Wei, F.; Deng, Q.-C.; Zheng, C.; Wan, C.-Y. *J. Mol. Catal. B: Enzym.* **2013**, *95*, 82−88. (c) Sorour, N.; Karboune, S.; Saint-Louis, R.; Kermasha, S. *J. Biotechnol.* **2012**, *158*, 128−136.
(23) (a) Weerasooriya, M. K. B.; Kumarasinghe, A. A. N. *Indian J. Chem. Techn.* **2012**, *19*, 244−249. (b) Jeon, J. H.; Kim, J. T.; Kim, Y. J.; Kim, H. K.; Lee, H. S.; Kang, S. G.; Kim, S. J.; Lee, J. H. *Appl. Microbiol. Biotechnol.* **2009**, *81*, 865−874. (c) Bajpai, D.; Tyagi, V. K. *J. Oleo Sci.* **2007**, *56*, 327−340.
(24) (a) Spinella, S.; Ganesh, M.; Lo Re, G.; Zhang, S.; Raquez, J. M.; Dubois, P.; Gross, R. A. *Green Chem.* **2015**, *17*, 4146−4150. (b) Düşkünkorur, H. Ö.; Bégué, A.; Pollet, E.; Phalip, V.; Güvenilir, Y.; Avérous, L. *J. Mol. Catal. B: Enzym.* **2015**, *115*, 20−28. (c) Yang, Y.; Zhang, J.; Wu, D.; Xing, Z.; Zhou, Y.; Shi, W.; Li, Q. *Biotechnol. Adv.* **2014**, *32*, 642−651. (d) Zhang, J.; Shi, H.; Wu, D.; Xing, Z.; Zhang, A.; Yang, Y.; Li, Q. *Process Biochem.* **2014**, *49*, 797−806.
(25) (a) Aouf, C.; Lecomte, J.; Villeneuve, P.; Dubreucq, E.; Fulcrand, H. *Green Chem.* **2012**, *14*, 2328−2336. (b) Jiang, Z. *Biomacromolecules* **2011**, *12*, 1912−1919. (c) Masoumi, H. R.; Kassim, A.; Basri, M.; Abdullah, D. K. *Molecules* **2011**, *16*, 4672−4680. (d) Jadhav, S. R.; Vemula, P. K.; Kumar, R.; Raghavan, S. R.; John, G. *Angew. Chem., Int. Ed.* **2010**, *49*, 7695−7698.
(26) (a) Poppe, J. K.; Fernandez-Lafuente, R.; Rodrigues, R. C.; Ayub, M. A. *Biotechnol. Adv.* **2015**, *33*, 511−525. (b) Kabbashi, N. A.; Mohammed, N. I.; Alam, M. Z.; Mirghani, M. E. S. *J. Mol. Catal. B: Enzym.* **2015**, *116*, 95−100. (c) Zhang, W.-W.; Yang, X.-L.; Jia, J.-Q.; Wang, N.; Hu, C.-L.; Yu, X.-Q. *J. Mol. Catal. B: Enzym.* **2015**, *115*, 83−89. (d) Liu, S.; Nie, K.; Zhang, X.; Wang, M.; Deng, L.; Ye, X.; Wang, F.; Tan, T. *J. Mol. Catal. B: Enzym.* **2014**, *99*, 43−50.
(27) Franssen, M. C.; Steunenberg, P.; Scott, E. L.; Zuilhof, H.; Sanders, J. P. *Chem. Soc. Rev.* **2013**, *42*, 6491−533.
(28) (a) Saranya, P.; Ramani, K.; Sekaran, G. *RSC Adv.* **2014**, *4*, 10680−10692. (b) Margesin, R.; Labbe, D.; Schinner, F.; Greer, C. W.; Whyte, L. G. *Appl. Environ. Microbiol.* **2003**, *69*, 3085−3092. (c) Margesin, R.; Zimmerbauer, G.; Schinner, F. *Biotechnol. Technol.* **1999**, *13*, 313−333.
(29) Mita, L.; Sica, V.; Guida, M.; Nicolucci, C.; Grimaldi, T.; Caputo, L.; Bianco, M.; Rossi, S.; Bencivenga, U.; Eldin, M. S. M.; Tufano, M. A.; Mita, D. G.; Diano, N. *J. Mol. Catal. B: Enzym.* **2010**, *62*, 133−141.
(30) (a) Samal, M.; Chercheja, S.; Rybacek, J.; Vacek Chocholousova, J.; Vacek, J.; Bednarova, L.; Saman, D.; Stara, I. G.; Stary, I. *J. Am. Chem. Soc.* **2015**, *137*, 8469−8474. (b) Lee, J.; Oh, Y.; Choi, Y. K.; Choi, E.; Kim, K.; Park, J.; Kim, M.-J. *ACS Catal.* **2015**, *5*, 683−689. (c) Lopez-Iglesias, M.; Busto, E.; Gotor, V.; Gotor-Fernandez, V. *J. Org. Chem.* **2015**, *80*, 3815−3824. (d) Rangel, H.; Carrillo-Morales, M.; Galindo, J. M.; Castillo, E.; Obregón-Zúñiga, A.; Juaristi, E.; Escalante, J. *Tetrahedron: Asymmetry* **2015**, *26*, 325−332.
(31) (a) Toledo, M. V.; José, C.; Collins, S. E.; Ferreira, M. L.; Briand, L. E. *J. Mol. Catal. B: Enzym.* **2015**, *118*, 52−61. (b) Schär, A.; Nyström, L. *J. Mol. Catal. B: Enzym.* **2015**, *118*, 29−35. (c) Quintana, P. G.; Canet, A.; Marciello, M.; Valero, F.; Palomo, J. M.; Baldessari, A. *J. Mol. Catal. B: Enzym.* **2015**, *118*, 36−42. (d) Lopresto, C. G.; Calabrò, V.; Woodley, J. M.; Tufvesson, P. *J. Mol. Catal. B: Enzym.* **2014**, *110*, 64−71.
(32) (a) Usui, K.; Yamamoto, K.; Shimizu, T.; Okazumi, M.; Mei, B.; Demizu, Y.; Kurihara, M.; Suemune, H. *J. Org. Chem.* **2015**, *80*, 6502−6508. (b) Rangel, H.; Carrillo-Morales, M.; Galindo, J. M.; Castillo, E.; Obregón-Zúñiga, A.; Juaristi, E.; Escalante, J. *Tetrahedron: Asymmetry* **2015**, *26*, 325−332. (c) Varga, A.; Naghi, M. A.; Füstös, M.; Katona, G.; Zaharia, V. *Tetrahedron: Asymmetry* **2014**, *25*, 298−304.
(33) Lopez-Iglesias, M.; Busto, E.; Gotor, V.; Gotor-Fernandez, V. *J. Org. Chem.* **2012**, *77*, 8049−8055.
(34) (a) Xia, B.; Li, Y.; Cheng, G.; Lin, X.; Wu, Q. *ChemCatChem* **2014**, *6*, 3448−3454. (b) Zheng, J.-Y.; Wang, Z.; Zhu, Q.; Zhang, Y.-J.; Yan, H.-D. *J. Mol. Catal. B: Enzym.* **2009**, *56*, 20−23.
(35) (a) Moni, L.; Banfi, L.; Basso, A.; Carcone, L.; Rasparini, M.; Riva, R. *J. Org. Chem.* **2015**, *80*, 3411−3428. (b) Namiki, Y.; Fujii, T.; Nakada, M. *Tetrahedron: Asymmetry* **2014**, *25*, 718−724. (c) Moni, L.; Banfi, L.; Basso, A.; Galatini, A.; Spallarossa, M.; Riva, R. *J. Org. Chem.* **2014**, *79*, 339−351. (d) Zheng, J.-Y.; Wang, S.-F.; Zhang, Y.-J.; Ying, X.-X.; Wang, Y.-g.; Wang, Z. *J. Mol. Catal. B: Enzym.* **2013**, *98*, 37−41. (e) Manzuna Sapu, C.; Bäckvall, J. E.; Deska, J. *Angew. Chem., Int. Ed.* **2011**, *50*, 9731−9734. (f) Garcia-Urdiales, E.; Alfonso, I.; Gotor, V. *Chem. Rev.* **2011**, *111*, PR110−PR180.
(36) Méndez-Sánchez, D.; Ríos-Lombardía, N.; García-Granda, S.; Montejo-Bernardo, J.; Fernández-González, A.; Gotor, V.; Gotor-Fernández, V. *Tetrahedron: Asymmetry* **2014**, *25*, 381−386.
(37) Rios-Lombardia, N.; Busto, E.; Gotor-Fernandez, V.; Gotor, V. *J. Org. Chem.* **2011**, *76*, 5709−5718.
(38) (a) Szczesniak, P.; Pazdzierniok-Holewa, A.; Klimczak, U.; Stecko, S. *J. Org. Chem.* **2014**, *79*, 11700−11713. (b) Radu, A.; Moisă, M. E.; Toşa, M. I.; Dima, N.; Zaharia, V.; Irimie, F. D. *J. Mol. Catal. B: Enzym.* **2014**, *107*, 114−119. (c) Klossowski, S.; Brodzka, A.; Zysk, M.; Ostaszewski, R. *Tetrahedron: Asymmetry* **2014**, *25*, 435−442. (d) Brem, J.; Bencze, L.-C.; Liljeblad, A.; Turcu, M. C.; Paizs, C.; Irimie, F.-D.; Kanerva, L. T. *Eur. J. Org. Chem.* **2012**, *2012*, 3288−3294.
(39) Selvig, K.; Ruud-Christensen, M.; Aasen, A. J. *J. Med. Chem.* **1983**, *26*, 1514−1518.
(40) Ruud-Christensen, M.; Salvesen, B. *J. Chromatogr.* **1984**, *303*, 433−435.
(41) Rice, R. V.; Heights, H. U.S. Patent 2,715,125, 1955.
(42) Chen, C. S.; Fujimoto, Y.; Girdaukas, G.; Sih, C. J. *J. Am. Chem. Soc.* **1982**, *104*, 7294−7299.
(43) (a) Kitamoto, Y.; Kuruma, Y.; Suzuki, K.; Hattori, T. *J. Org. Chem.* **2015**, *80*, 521−527. (b) Petrenz, A.; María, P. D. d.; Ramanathan, A.; Hanefeld, U.; Ansorge-Schumacher, M. B.; Kara, S.

DOI: 10.1021/acs.joc.5b01840
J. Org. Chem. 2016, 81, 380−395

J. Mol. Catal. B: Enzym. **2015**, *114*, 42−49. (c) Godoy, C. A.; Fernández-Lorente, G.; de las Rivas, B.; Filice, M.; Guisan, J. M.; Palomo, J. M. *J. Mol. Catal. B: Enzym.* **2011**, *70*, 144−148.
(44) (a) Wikmark, Y.; Svedendahl Humble, M.; Bäckvall, J. E. *Angew. Chem., Int. Ed.* **2015**, *54*, 4284−4288. (b) Corici, L.; Pellis, A.; Ferrario, V.; Ebert, C.; Cantone, S.; Gardossi, L. *Adv. Synth. Catal.* **2015**, *357*, 1763−1774. (c) Ferrari, F.; Paris, C.; Maigret, B.; Bidouil, C.; Delaunay, S.; Humeau, C.; Chevalot, I. *J. Mol. Catal. B: Enzym.* **2014**, *101*, 122−132. (d) Escorcia, A. M.; Daza, M. C.; Doerr, M. *J. Mol. Catal. B: Enzym.* **2014**, *108*, 21−31. (e) Baum, I.; Elsässer, B.; Schwab, L. W.; Loos, K.; Fels, G. *ACS Catal.* **2011**, *1*, 323−336.
(45) Trott, O.; Olson, A. J. *J. Comput. Chem.* **2010**, *31*, 455−461.
(46) (a) Dodson, G. *Trends Biochem. Sci.* **1998**, *23*, 347−352. (b) Uppenberg, J.; Oehrner, N.; Norin, M.; Hult, K.; Kleywegt, G. J.; Patkar, S.; Waagen, V.; Anthonsen, T.; Jones, T. A. *Biochemistry* **1995**, *34*, 16838−16851. (c) Derewenda, Z. S.; Derewenda, U. *Biochem. Cell Biol.* **1991**, *69*, 842−851. (d) Brady, L.; Brzozowski, A. M.; Derewenda, Z. S.; Dodson, E.; Dodson, G.; Tolley, S.; Turkenburg, J. P.; Christiansen, L.; Huge-Jensen, B.; Norskov, L.; Thim, L.; Menge, U. *Nature* **1990**, *343*, 767−770.
(47) Uppenberg, J.; Hansen, M. T.; Patkar, S.; Jones, T. A. *Structure* **1994**, *2*, 293−308.
(48) Williams, D. B. G.; Lawton, M. *J. Org. Chem.* **2010**, *75*, 8351−8354.
(49) Pettersen, E. F.; Goddard, T. D.; Huang, C. C.; Couch, G. S.; Greenblatt, D. M.; Meng, E. C.; Ferrin, T. E. *J. Comput. Chem.* **2004**, *25*, 1605−1612.
(50) Sanner, M. F. *J. Mol. Graph. Model.* **1999**, *17*, 57−61.

DOI: 10.1021/acs.joc.5b01840
J. Org. Chem. 2016, 81, 380−395